



UvA-DARE (Digital Academic Repository)

Influence of immunoglobulin G-glycan and subclass variation on antibody effector functions

Dekkers, G.

Publication date

2017

Document Version

Other version

License

Other

[Link to publication](#)

Citation for published version (APA):

Dekkers, G. (2017). *Influence of immunoglobulin G-glycan and subclass variation on antibody effector functions*.

General rights

It is not permitted to download or to forward/distribute the text or part of it without the consent of the author(s) and/or copyright holder(s), other than for strictly personal, individual use, unless the work is under an open content license (like Creative Commons).

Disclaimer/Complaints regulations

If you believe that digital publication of certain material infringes any of your rights or (privacy) interests, please let the Library know, stating your reasons. In case of a legitimate complaint, the Library will make the material inaccessible and/or remove it from the website. Please Ask the Library: <https://uba.uva.nl/en/contact>, or a letter to: Library of the University of Amsterdam, Secretariat, Singel 425, 1012 WP Amsterdam, The Netherlands. You will be contacted as soon as possible.



IgG hexamerization

Decoding the human IgG-glycan repertoire reveals a spectrum of Fc-receptor- and complement-mediated- effector activities

Gillian Dekkers¹, Louise Treffers², Rosina Plomp³, Arthur E.H. Bentlage¹, Marcella de Boer¹, Carolien A.M. Koeleman³, Suzanne L. Lissenberg-Thunnissen¹, Remco Visser¹, Mieke Brouwer⁴, Juk Yee Mok⁵, Hanke Matlung², Timo van den Berg², Wim J.E. van Esch⁵, Taco Kuijpers², Diana Wouters⁴, Theo Rispens⁴, Manfred Wuhrer³, Gestur Vidarsson¹

¹ Sanquin Research and Landsteiner Laboratory, Department Experimental Immunohematology, Academic Medical Centre, University of Amsterdam, Amsterdam, The Netherlands

² Sanquin Research and Landsteiner Laboratory, Department Blood Cell Research, Academic Medical Centre, University of Amsterdam, Amsterdam, The Netherlands

³ Center for Proteomics and Metabolomics, Leiden University Medical Center, Leiden, The Netherlands

⁴ Sanquin Research and Landsteiner Laboratory, Department Immunopathology, Academic Medical Centre, University of Amsterdam, Amsterdam, The Netherlands

⁵ Sanquin Reagents, Amsterdam, The Netherlands.

ABSTRACT

3

Glycosylation of the immunoglobulin G (IgG)-Fc tail is required for binding to Fc-gamma receptors (FcγRs) and complement-component C1q. A variety of IgG1 glycoforms is detected in human sera. Several groups have found global or antigen specific skewing of IgG glycosylation, for example in autoimmune diseases, viral infections, and alloimmune reactions. The IgG glycoprofiles seem to correlate with disease outcome. Additionally, IgG-glycan composition contributes significantly to Ig based therapies, as for example IVIg in autoimmune diseases and therapeutic antibodies for cancer treatment. The effect of the different glycan modifications, especially of fucosylation, has been studied before. However the contribution of the 20 individual IgG glycoforms, in which the combined effect of all four modifications, to the IgG function has never been investigated. Here we combined six glyco-engineering methods to generate all 20 major human IgG1 glycoforms and screened their functional capacity for FcγR- and complement activity. Bisection had no effect on FcγR or C1q-binding, and sialylation had no- or little effect on FcγR-binding. We confirmed that hypo-fucosylation of IgG1 increased binding to FcγRIIIa and FcγRIIIb by ~17-fold, but in addition we showed that this effect could be further increased to ~40-fold for FcγRIIIa upon simultaneous hypo-fucosylation and hyper-galactosylation, resulting in enhanced NK-cell mediated antibody-dependent cellular-cytotoxicity (ADCC). Moreover, elevated galactosylation and sialylation significantly increased (independent of fucosylation) C1q-binding, downstream complement deposition, and cytotoxicity. In conclusion, fucosylation and galactosylation are primary mediators of functional changes in IgG for FcγR- and complement-mediated effector functions, respectively, with galactose having an auxiliary role for FcγRIII-mediated functions. This knowledge could be used for glycan profiling of clinically important (antigen-specific) IgG, but also to optimize therapeutic antibody applications.

Introduction

The importance of the biological properties of antibodies to specifically engage a target of choice and activate complement and Fc gamma receptors (FcγR) on immune cells¹ is currently more and more recognized in modern medicine. For cancer therapies using tumor targeting antibodies, strong effector functions are preferred². Various strategies have been exploited to generate antibodies that are more effective than wild-type human IgG1 isotype³. These include fusions with toxic molecules and incorporations of mutations that enhance affinities to FcγR. Possible drawbacks of such modifications is the introduction of foreign immunogenic epitopes that can result in anti-drug antibodies that may neutralize the drug. This can be circumvented by using non-immunogenic natural variations, found in all individuals. The prototypic variation of this kind are glyco-engineered IgG1 antibodies without fucose with elevated FcγRIIIa affinities^{4,5}, which have already found its way to therapeutic antibodies on the market⁶.

This fucose residue is part of a conserved glycan on asparagine 297 in the Fc domain of IgG. This glycan is important for the quaternary structure of the Fc part, since its removal abrogates binding of FcγR and C1q and hence the antibody's effector functions⁷⁻⁹. In addition to affecting the Fc structure and thereby recognition by these effector molecules, the Fc-glycan also affects binding to FcγRIIIa and FcγRIIIb through a glycan-glycan interaction^{10,11}. This is because of a unique glycan found in human FcγRIIIa and FcγRIIIb at position 162 that interacts directly with the Fc-glycan within the IgG-Fc-cavity¹¹.

The N297 glycan is a bi-antennary complex glycan composed of a constant part with a core consisting of *N*-acetylglucosamines and mannoses and can be found in human serum with variable levels of core fucose, bisecting *N*-acetylglucosamine, galactose and terminal sialic acids¹². The N-glycans of total serum/plasma IgG consists on average of high fucose levels (95%), low bisection (15%), intermediate levels of galactose (45%), and low sialic acid (10%)¹². The variable assembly of the glycans amounts to at least 20 different glycoforms (a term used here to describe one unique glycan combination) for each IgG-subclass being found in serum, with ~8 of them accounting for 90% of the total abundance¹². The composition of total IgG glycosylation can change upon certain settings, where galactosylation and sialylation increase with pregnancy^{12,13}. Changes in total IgG are also observed in various clinical settings, with a low level of galactosylation and sialylation is associated both with increasing age and autoimmune diseases¹²⁻¹⁵.

We and others have shown that IgG-Fc-glycosylation changes of antigen-specific IgG can occur that correlate with disease outcome¹⁶⁻²⁰. This includes both auto- and alloimmune disorders, including fetal neonatal immune thrombocytopenia (FNAIT), immune thrombocytopenia (ITP), and hemolytic disease of the fetus and newborn (HDFN)^{16-18,21,22}. In particular, we have found that immune responses against red blood cell (RBC) and platelets, either transfused or during pregnancy, can be characterized with extremely low fucose (down to 10%), high galactose (up to 80%) and elevated sialylation

levels (~35%). Notably, lowered Fc-fucosylation,^{17,21} but also elevated Fc-galactosylation¹⁸, seemed to correlate with elevated blood cell destruction, severity of anemia or bleeding for red blood cells and platelets respectively. Whereas the increased pathogenicity associated with lowered fucosylation could be explained by the resulting elevated FcγRIIIa and/or FcγRIIIb activity^{17,23}, the functional reasons – if any – behind the association with elevated galactosylation remained enigmatic.

The effect of Fc-bisection and -sialylation on human FcγR binding, if any, has been studied in even less detail, although binding to the human FcγRIIIa does not seem to be affected by sialylation²⁴. Whether these glycan changes influence binding to C1q, and subsequent complement activation, has not been studied in detail^{25,26}. A drawback of all these studies is that the impact of the glycan changes were studied changing only individual end groups, without investigating the possibility that the context of the other glycan changes may have an effect on the antibody effector functions.

The complexity of the glycan-assembly makes investigation into their biological relevance extremely difficult. Previous attempts have generated a handful of defined glycoforms and tested binding to part of the FcγR-repertoire, but a systematic analysis for all possible glycan changes and effector mediators, FcγRs and complement, has never been achieved^{24,26–30}. This information could provide the insight in working mechanisms of IgG based treatments and allow meaningful clinical evaluation of the activity of potentially pathological antibodies such as in FNAIT and HDFN. We have therefore developed a set of glyco-engineering tools which specifically alter one of the N-glycan end groups³¹ and in the present study we combined these tool to create 20 different natural glycoforms to systematically investigate them with regard to FcγR binding, ADCC, complement binding and activation.

Material and Methods

Human Samples. Peripheral blood from anonymous, healthy volunteers was obtained with informed, written consent in accordance with Dutch regulations. This study was approved by the Sanquin Ethical Advisory Board in accordance with the Declaration of Helsinki.

Heparinized blood samples were used for isolation of peripheral blood mononuclear cells (PBMCs) or red blood cells (RBCs). NK cell isolation was only performed with blood from well-genotyped donors that do not express FcγRIIc³² to exclude any possible effects of this receptor. Serum was obtained by allowing blood without anticoagulants to coagulate for 1 hour at room temperature (RT) and collecting the supernatant after centrifugation at 950 g for 10 min. Serum of three different volunteers was combined to create a serum pool.

Strains and reagents. Escherichia coli strain DH5α was used for recombinant DNA work. Restriction endonucleases, DNA modification enzymes were obtained from Thermo Fisher Scientific (Waltham, Massachusetts, USA). Oligonucleotides were obtained from Genart (Thermo Fisher Scientific) or Integrated DNA Technologies (Coralville, Iowa, USA).

IgG1 expression vector constructs. Variable (V) genes for anti-human RhD (anti-D clone 19A10) heavy and light chain were sequenced from a single human B cell from a hyper immunized donor³³. A single-gene vector containing anti-D or anti-TNP IgG1 heavy- and kappa-light chain encoding sequences were cloned as described previously by Kruijssen et al.³⁴ into a pEE14.4 (Lonza, Basel, Switzerland) expression vector. For both anti-TNP and anti-D IgG a single expression vector was generated. In brief, the codon-optimized V gene for both heavy and light chain, including 5'-HindIII and 3'-NheI or 5'-HindIII and 3'-XhoI restriction sites respectively, Kozak sequence, and HAVT20-leader sequence, were designed and ordered from Geneart (Thermo Fisher Scientific). The HindIII-NheI or HindIII-XhoI fragments for the codon-optimized heavy or light chain were ligated into γ or κ constant region flanking 3'-EcoRI restriction site respectively. The HindIII-EcoRI fragment for the codon-optimized light chain was ligated into pEE14.4 (Lonza), and the HindIII-EcoRI fragment for the heavy chain was ligated into pEE6.4 (Lonza). A single-gene vector encoding IgG1 was subsequently generated by ligation of the BamHI-NotI fragment from pEE6.4 (including a cytomegalovirus (CMV) promoter), IgG1 heavy chain, and poly (A) into the light-chain-encoding pEE14.4 vector.

IgG1 production and glyco-engineering. IgG1 production in HEK F cells and purification using protein A affinity chromatography was performed as described previously by Kruijssen et al.³⁴ Glyco-engineering of IgG1 was optimized as described by Dekkers et al.³¹ In short: To decrease either fucosylation or galactosylation 0.4 mM 2-deoxy-2-fluoro-l-fucose (2FF) (Carbosynth, Berkshire, United Kingdom) or 1 mM 2-deoxy-2-fluoro-d-galactose (2FG) (Carbosynth) respectively was added to the cell suspension 4 hours post transfection. To increase bisecting GlcNAc, 1% pEE6.4+GNTIII encoding mannosyl (beta-1,4-)-glycoprotein beta-1,4-N-acetylglucosaminyltransferase (GNTIII) enzyme was co-transfected with 99% IgG1- κ HC+LC vector. To increase galactose, 1% pEE6.4+B4GALT1 encoding β -1,4-galactosyltransferase 1 (B4GALT1) enzyme was co-transfected with 99% IgG1 vector and 5 mM D-galactose (Sigma Aldrich, Saint Louis, Missouri, USA) was added to the cell suspension 1 hour before transfection. To increase sialylation, the level of galactosylation must also be elevated as sialic acid is the terminal sugar group with galactose residues as substrate. Thus, 1% pEE6.4+B4GALT1 and 2.5% pEE14.4+STGALT encoding β -galactoside alpha-2,6-sialyltransferase 1 (ST6GALT) were both co-transfected 96.5% IgG1 vector and 5 mM D-galactose was added to the cell suspension 1 hour before transfection. To further increase sialylation, *in vitro* sialylation (*ivs*) was performed on the purified *in vivo* sialylated IgG created using the previous method. Recombinant human α -2,6-sialyltransferase (Roche, Basel, Switzerland) and cytidine-5'-monophospho-N-acetylneuraminic acid (CMP-NANA) (Roche) were incubated at 37 °C for 24 hours with purified IgG1 with already *in vivo* enhanced galactose and sialic acid (as described above), after incubation samples were re-purified with protein A, as described previously^{31,34}.

Mass spectrometry analysis. IgG Fc glycan composition of produced IgG1 was determined by mass spectrometry as described previously by Dekkers et al.³¹ Trypsin-digested glycopeptide samples were analyzed by nanoLC-ESI-QTOF-MS. The separation was performed on an RSLCnano Ultimate 3000 system (ThermoFisher, Breda, the Netherlands) with a gradient pump, loading pump and an autosampler. 250 nl of sample was injected and washed on a Dionex Acclaim PepMap100 C18 trap

column (5 mm × 300 μm i.d.; ThermoFisher) for 1 min with 0.1% TFA at a flow rate of 25 μl/min. The sample was then separated on an Ascentis Express C18 nanoLC analytic column (50 mm × 75 μm i.d.; 2.7 μm fused core particles; Supelco, Bellefonte, PA) with a flow rate of 0.9 μl/min using linear gradient as described in³¹. The resulting co-elution of the different glycoforms of the IgG1 Fc glycosylation site warrants fair comparison by ensuring identical ionization conditions for the various glycopeptide species. The LC was coupled to the MS detector via a CaptiveSpray source with a NanoBooster (Bruker Daltonics, Bremen, Germany). The latter enriched the N₂ flow (3 L/min) with CH₃CN (pressure 0.2bar), resulting in increased sensitivity. The samples were ionized in positive ion mode at 1100 V. The Maxis Impact quadrupole-TOF-MS (microTOF-Q, Bruker Daltonics) was used as detector. MS1 spectra were collected at a frequency of 1 Hz with a scan range of *m/z* 550-1800. The mass spectrometric data was calibrated internally in DataAnalysis 4.0 (Bruker Daltonics) using a list of known IgG glycopeptide masses. MSConvert (Proteowizard 3.0)³⁵ was used to convert the data files to mzXML format, and an in-house alignment tool³⁶ was used to align the retention times of the data files. The highest intensity of selected peaks (within an *m/z* window of +/-0.2 and within a time window of +/-15 s surrounding the retention time) was extracted using the in-house developed 3D Max Xtractor software tool. If above a signal:background ratio of 3, the background-subtracted area of the first 3 isotopic peaks of each glycopeptide in both 2+, 3+ and 4+ charge state were summed, and this summed value was then divided by the total summed value of all IgG1 glycopeptides to arrive at a percentage for each glycopeptide. From these percentages we calculated several derived traits using the following formulas: fucosylation (H3N3F1 + H4N3F1 + H5N3F1 + H6N3F1 + G0F + G1F + G2F + H6N4F1 + G0FN + G1FN + G2FN + H6N5F1 + H4N3F1S1 + H5N3F1S1 + H6N3F1S1 + G1FS + G2FS + H6N4F1S1 + G2FS2 + G1FNS + G2FNS + H6N5F1S1 + G2FNS2), bisection (H6N4F1 + G0FN + G1FN + G2FN + H6N5F1 + H6N4F1S1 + G1FNS + G2FNS + H6N5F1S1 + G2FNS2 + H6N4 + G0N + G1N + G2N + H6N5 + H6N4S1 + G1NS + G2NS + H6N5S1 + G2NS2), galactosylation ((H4N3F1 + H5N3F1 + G1F + H6N4F1 + G1FN + H6N5F1 + H4N3F1S1 + H5N3F1S1 + H6N3F1S1 + G1FS + H6N4F1S1 + G1FNS + H6N5F1S1 + H4N3 + H5N3 + H6N3 + G1 + H6N4 + G1N + H6N5 + H4N3S1 + H5N3S1 + H6N3S1 + G1S + H6N4S1 + G1NS + H6N5S1) * 0.5 + G2F + G2FN + G2FS + G2FS2 + G2FNS + G2FNS2 + G2 + G2N + G2S + G2S2 + G2NS + G2NS2), sialylation ((H4N3F1S1 + H5N3F1S1 + H6N3F1S1 + G1FS + G2FS + H6N4F1S1 + G1FNS + G2FNS + H6N5F1S1 + H4N3S1 + H5N3S1 + H6N3S1 + G1S + G2S + H6N4S1 + G1NS + G2NS + H6N5S1) * 0.5 + G2FS2 + G2FNS2 + G2S2 + G2NS2), hybrid-types (H5N3F1 + H6N3F1 + H6N4F1 + H6N5F1 + H5N3F1S1 + H6N3F1S1 + H6N4F1S1 + H6N5F1S1 + H5N3 + H6N3 + H6N4 + H6N5 + H5N3S1 + H6N3S1 + H6N4S1 + H6N5S1) and high-mannose (H5N2 + H6N2 + H7N2 + H8N2 + H9N2). For some of the minor hybrid-type glycans it could not be determined conclusively whether a galactose or a bisecting *N*-acetylglucosamine was present, so an educated guess was made based on structural knowledge (for instance, since the hybrid glycan H6N4F1 is elevated in GNTIII-co-transfected HEK cell-derived IgG samples, it is likely to be a bisected species rather than triantennary).

High-performance liquid chromatography HPLC. Protein A purified IgG was analyzed for monomeric and dimeric IgG on a Superdex 200 10/300 gel filtration column (30 cm, 24 ml, 17-15175-01, GE Healthcare, Little Chalfont, United Kingdom) connected to an Äkta explorer (GE Healthcare)

HPLC system at room temperature with a flow rate of 0.5 ml/min and PBS as running buffer. Elution profiles were obtained by recording the absorbance at 215 nm.

Human FcγR constructs. Human FcγR constructs (FcγRIa (HIS tag), FcγRIIa (131His, Biotinylated, and 131Arg, Biotinylated), FcγRIIb (Biotinylated), FcγRIIIa (158Phe, Biotinylated, and 158Val, Biotinylated) and FcγRIIIb (NA2, HIS tag)), for SPR analysis were obtained from Sino biological (Beijing, China). To further include all human FcγRs a fusion Fc-FcγR construct composed of the extracellular domain of the FcγRIIIb in both allotypes followed by a Fc domain was created. To create the fusion Fc-FcγRIIIb constructs the amino acid code of the extracellular domain of either FcγRIIIb of NA1 allotype or FcγRIIIb NA2 allotype³⁷ (NCBI reference sequence NP_000561.3), and IgG2 Fc domain, composed of a human IgA1a hinge, human IgG2 Fc CH2 and CH3 domains including mutations deleting the Fc-glycan (N297A) and introducing a C-terminal biotinylation tag (BirA) were reverse translated and codon optimized at Geneart. DNA was ordered (Integrated DNA technologies, Coralville, IA, USA) and cloned into pcDNA3.1 (Invitrogen, Carlsbad, California, USA) expression vector using flanking HindIII and EcoRV restriction sites. A model of the construct and sequences are displayed in **Supplementary Fig. 7a-b**. The construct was produced and purified as described previously³¹. After purification the protein was site-specifically biotinylated on the BirA tag using BirA enzyme as described by Rodenko et al.³⁸. For biotinylation of 1 μM FcγR protein 0.00657 μM BirA ligase was used. After biotinylation overnight at 25 °C the FcγR sample was buffer-exchanged and subsequently concentrated in PBS pH 7.4 using Amicon Ultra centrifugal filter units (MWCO 30 kDa) (Merck, Millipore, Darmstadt, Germany). The quality of the Fc-Fusion receptors was confirmed by comparing the binding of normally glycosylated IgG1 to the acquired his-tagged receptor (Sino-biological) and in house made Fc-Fusion of the same allotype (NA2) (**Supplementary Fig. 7c-d**).

Surface plasmon resonance. SPR measurement were performed as described by Dekkers et al.³⁹. All biotinylated FcγR were spotted using a Continuous Flow Microspotter (Wasatch Microfluidics, Salt Lake City, UT) onto a single SensEye G-streptavidin sensor (Ssens, Enschede, Netherlands) allowing for binding affinity measurements of each antibody to all FcγR simultaneously on the IBIS MX96 (IBIS Technologies, Enschede, Netherlands) as described by de Lau et al.⁴⁰. The biotinylated FcγRs were spotted in three-fold dilutions, ranging from 100 nM to 3 nM for FcγRIIb and fusion FcγRIIIb-IgG2-Fc. All the other FcγRs were spotted in three-fold dilutions, ranging from 30 nM to 1 nM in PBS 0.0075% Tween-80 (Amresco), pH 7.4. The IgGs were then injected over the IBIS at 1.5 dilution series starting at 5.9 nM until 506.25 nM or 0.9 nM until 2000 nM, when necessary, in PBS in 0.075% Tween-80. For FcγRI affinity and FcγRIIIb control measurements his-tagged FcγRI or FcγRIIIb was used. Biotinylated anti-His-tagged antibody (Genscript Piscataway, New Jersey, USA) was spotted in three-fold dilutions, ranging from 30 nM to 1 nM. Before every IgG injection 50 nM his-tagged FcγR was injected. The IgGs were then injected over the IBIS at 3 fold dilution series starting at 0.41 nM until 100 nM for FcγRI and 94 nM until 3000 nM for FcγRIIIb. Regeneration after every sample was carried out with acid buffer (10 mM Gly-HCl, pH 2.4). Calculation of the dissociation constant (K_D) was done using an equilibrium analysis by linear intrapolation to $R_{max}=500^{41}$. Analysis and calculation of all binding data was carried out with Scrubber software version 2 (Biologic Software, Campbell, Australia) and Microsoft Office

B4GALT1 co-transfection and 5 mM D-galactose, ST6GALT – 2.5% ST6GALT co-transfection, *in vitro* sial treatment of IgG with recombinant ST6GALT and CMP-NANA substrate. The data represents the mean and SEM of at least 2 combined independent experiments; *, **, *** and **** denote a statistical significance of $p \leq 0.05$, $p \leq 0.01$, $p \leq 0.001$ and $p \leq 0.0001$, respectively, as tested by one-way ANOVA against unmodified IgG1, using Dunnett's multiple comparisons test. U: Unmodified glycoform.

Excel 2013.

NK cell mediated ADCC. NK cells were isolated from Ficoll-Plaque™-Plus (GE Healthcare) gradient obtained PBMCs by a CD56 magnetic-activated cell separation (MACS) isolation kit (Miltenyi Biotec, Leiden, The Netherlands), according to manufacturer's description. D+ red blood cells (RBC) were isolated and labeled with radioactive chromium ($100 \mu\text{Ci } ^{51}\text{Cr}$, PerkinElmer, Waltham, Massachusetts, USA) at 10^9 cells/ml. An amount of 10^5 erythrocytes were incubated with NK cells for 2 hours at 37 °C in a 2:1 ratio in Iscove's modified dulbecco's medium (IMDM, Gibco, Thermo Fisher Scientific) supplemented with 10% fetal calf serum (FCS, Bodinco, Alkmaar, The Netherlands) and anti-D IgG1 glycoforms at a total volume of 100 μl . To determine 100% lysis, 2.5% saponine (Fluka, Sigma Aldrich) was added to RBC in control wells and spontaneous lysis (sp) was determined by incubation of RBC without NK cells. Supernatants were collected and released ^{51}Cr was quantified in a Packard Cobra II Auto-Gamma Counter Model D5005 (PerkinElmer). Percentage cytotoxicity was determined by the following formula:

$$\text{ADCC (\%)} = \frac{(\text{counts sample} - \text{counts sp})}{(\text{counts 100\%} - \text{counts sp})} \times 100$$

Each value consisted of at least 3 individual sample wells.

Complement deposition ELISA. A 2.4 mM 2,4,6-trinitrobenzenesulfonic acid (TNBS) (Sigma-Aldrich) solution was added to 20 mg human serum albumin (HSA) diluted to 20 mg/ml (Sanquin, Amsterdam, The Netherlands) in 0.2 M Na_2HPO_4 (Merck, Millipore) and incubated 30 min at RT. To remove unbound TNBS, the solution was dialyzed (1:2000) using a dialysis cassette (Thermo Fisher Scientific Slide-A-Lyzer G2 cassette, 10K MWCO) for 1.5 hour at RT against PBS and additionally overnight at 4 °C to obtain HSA-TNP.

To coat, maxisorp plates (Thermo Scientific, Nunc flat-bottom 96 well plate) were incubated o/n at RT with 20 $\mu\text{g/ml}$ HSA-TNP in PBS. The plates were washed 5x with PBS + 0.1% tween-20 (Sigma-Aldrich) (wash buffer) using an ELISA washer (Biotek, 405 LSRS). All following washing steps were done similarly. The IgG samples were diluted in 100 μl PBS/plx (PBS + 0.1% poloxamer (Sigma-Aldrich, poloxamer 407)) per well and incubated for 1.5 hour at RT. The plates were washed and incubated with 100 μl 1:35 serum pool in VB+ / plx (veronalbuffer (3 mM Barbital (Sigma-Aldrich), 1.8 mM Sodium-Barbital (Sigma Aldrich), 0.146 M NaCl (Fagron, Capelle aan den IJssel, The Netherlands), pH 7.4) + 10 mM CaCl_2 (Merck) + 2 mM MgCl_2 (Merck) + 0.1% poloxamer) for 1 hour at RT. When C1q was blocked, 10 minutes prior to addition of serum to the ELISA plate, anti-C1q-85 blocking antibody⁴² was added to the VB+ / plx + 1:35 serum solution in a 1:2 molar ratio of C1q:anti-C1q-85 with final concentration of 8.57 $\mu\text{g/ml}$ anti-C1q-85. The plates were washed and 100 μl with either 2 $\mu\text{g/ml}$ biotinylated anti-C1q-2⁴², 0.5 $\mu\text{g/ml}$ biotinylated anti-C4-10⁴³, 0.6 $\mu\text{g/ml}$ biotinylated anti-C3-19⁴⁴, or 1 $\mu\text{g/ml}$ HRP labelled anti-human IgG (Sanquin, Pelicclass) in PBS/plx was added to respectively detect C1q, C4b, C3b or IgG deposition and incubated for 1 hour at RT. The plates were washed, C1q, C4b

Supplementary table 1. Comprehensive list of the IgG1 N-glycans which were detected during data analysis.

2FF (0.4 mM 2-deoxy-2-fluoro-L-fucose), 2FG (1 mM 2-deoxy-2-fluoro-D-galactose), GNT3 (co-transfection of 1% GNT3 vector), B4GALT1/D-galactose (co-transfection of 1% B4GALT1 vector and addition of 5 mM D-galactose), ST6GALT (co-transfection of 2.5% ST6GALT vector), and *in vitro* sialylation (treatment of sample with recombinant ST6GALT and CMP-NANA). These resulted in significantly different glycosylation traits (fucosylation, bisection, galactosylation, sialylation, high-mannose, hybrid-type), which are calculated from the relative abundances of individual N-glycans.

name	glyco-engineering		relative abundance glycopeptides*																									
	2FF (-)	2FG (-G)	GNT3 (+B)	B4GALT1/D-galactose (+G)	ST6GALT (+S)	in vitro sialylation (+ivs)	G0F	G1F	G2F	G0FN	G1FN	G2FN	G0NS2	G1NS2	G2NS2	G0S	G1S	G2S	G0SN2	G1SN2	G2SN2	SNTG	SZNG	ZSNG				
anti-D																												
-G	-	72.7	12.7	1.2	1.6	0.4	0.0	0.2	0.4	0.1	0.0	0.0	0.0	0.0	0.0	0.9	0.8	0.1	0.1	0.1	0.0	0.1	0.0	0.0	0.0	0.0		
Unmodified	-	37.5	37.7	9.8	1.8	2.6	0.4	0.7	1.5	0.7	0.1	0.1	0.0	0.1	0.0	0.1	0.8	0.7	0.2	0.3	0.1	0.6	0.3	0.2	0.1	0.0	0.1	
+G	-	2.3	7.6	54.6	0.1	1.0	0.9	0.1	11.7	4.0	0.2	0.1	0.0	0.0	0.1	0.0	0.0	0.1	0.4	0.0	0.0	0.5	0.4	0.8	0.2	0.0	0.1	0.0
+G+S	-	4.2	10.0	14.2	0.1	0.5	0.3	3.2	35.0	19.9	0.5	0.3	0.1	0.1	0.1	0.1	0.2	0.0	0.0	0.1	0.1	0.5	0.3	0.0	0.3	0.2	0.2	
+G+S+HvS	-	3.8	2.9	0.2	0.2	0.1	0.1	10.4	14.2	51.8	0.7	0.2	0.6	0.3	0.4	0.1	0.1	0.0	0.0	0.0	0.5	0.8	1.4	0.2	0.1	0.3	0.2	
-G+B	-	11.5	8.8	9.3	46.2	5.7	0.1	0.0	0.0	0.0	0.1	0.0	0.0	0.0	0.5	0.8	2.8	1.2	1.2	1.2	0.1	0.1	0.0	0.0	0.0	0.0	0.0	
+B	-	4.8	8.5	11.3	26.1	33.0	3.1	0.2	0.5	0.0	1.1	0.6	0.1	0.1	0.6	0.1	0.3	2.0	0.2	0.4	0.4	0.1	0.1	0.0	0.2	0.1	0.0	
+B+G	-	1.0	2.9	13.0	1.4	16.5	26.4	0.2	3.2	0.8	0.4	4.1	1.9	0.0	0.1	0.4	0.0	0.1	0.4	0.0	0.1	0.6	0.1	0.3	0.1	0.3	0.4	0.1
+B+G+S	-	2.4	5.1	5.4	2.6	10.9	5.6	1.7	12.1	7.1	12.4	6.9	9.9	0.2	0.2	0.6	0.0	0.1	0.3	0.1	0.3	0.1	0.3	0.2	0.2	0.5	0.2	
+B+G+S+HvS	-	2.3	1.8	1.2	2.4	0.7	0.2	5.0	5.4	17.8	21.7	0.6	20.3	0.3	0.3	0.7	0.2	0.1	0.0	0.3	0.4	0.7	0.9	0.7	0.7	0.7	0.7	
-F-G	+	20.4	4.9	1.2	0.6	0.3	0.1	0.1	0.7	0.2	0.1	0.0	0.0	0.0	52.7	6.1	0.4	0.8	0.2	0.0	0.1	0.1	0.1	0.0	0.1	0.0	0.0	
-F	+	11.4	13.3	3.9	0.5	0.8	0.1	0.3	0.6	0.5	0.1	0.0	0.1	0.0	30.6	23.5	5.1	1.0	1.2	0.2	0.5	0.7	0.4	0.1	0.1	0.1	0.1	
-F+G	+	0.6	2.2	15.7	0.5	0.2	0.2	0.1	3.3	1.5	0.0	0.0	0.0	0.0	2.4	7.4	42.7	0.1	0.6	0.6	0.2	6.4	2.3	0.1	0.0	0.0	0.0	
-F+G+S	+	1.5	3.0	3.0	0.1	0.1	0.1	1.3	8.9	5.3	0.1	0.1	0.0	0.1	5.6	11.9	6.8	0.1	0.3	0.2	6.0	24.2	10.8	0.2	0.2	0.1	0.1	
-F+G+S+HvS	+	1.5	1.0	0.4	0.1	0.1	0.1	3.3	2.8	12.6	0.2	0.2	0.0	0.2	5.2	4.3	0.2	0.1	0.2	0.2	14.0	11.4	31.5	0.3	0.3	0.2	0.2	
-F+G+B	+	4.3	3.0	2.3	16.1	2.6	0.1	0.0	0.0	0.1	0.0	0.0	0.0	0.0	9.6	5.8	7.9	34.9	2.9	0.1	0.0	0.0	0.0	0.0	0.1	0.0	0.1	
-F+B	+	1.8	3.0	2.5	8.8	11.5	1.1	0.1	0.2	0.1	0.5	0.3	0.1	4.3	5.6	8.4	24.4	18.9	1.4	0.1	0.2	0.0	0.7	0.3	0.1	0.1	0.1	
-F+B+G	+	0.4	1.2	5.0	0.7	5.6	9.1	0.3	1.1	0.4	0.2	1.7	0.8	1.0	2.5	10.5	1.3	14.8	16.4	0.2	1.8	0.5	0.3	2.5	0.9	0.9	0.9	
-F+B+G+S	+	0.7	1.6	1.9	1.0	3.8	2.4	0.5	4.4	2.5	3.5	2.5	3.8	2.1	4.1	3.6	2.2	9.0	3.5	1.8	9.7	4.5	8.6	4.1	4.9	4.9		
-F+B+G+S+HvS	+	0.8	0.7	0.4	0.9	0.3	0.5	1.5	1.8	6.0	7.2	0.3	7.5	2.0	1.7	1.0	2.0	0.7	0.1	4.3	5.2	12.2	17.1	0.7	11.4	11.4		

and C3 plates were incubated with 100 μ l 0.2 μ g/ml strep-poly HRP (Sanquin, Peliclass) (C1q) or 0.25 μ g/ml strep-HRP (Sigma-Aldrich) (C4b and C3b) in PBS/plx for 1 hour at RT. The plates were washed and developed for 5-10 minutes using 100 μ l TMB mix composed of 0.11 M NaAc (pH 5.5) (Merck), 0.1 mg/ml 3,3',5,5'-Tetramethylbenzidine (Merck) and 0.003 % H₂O₂ (Merck) and the reaction was stopped with the addition of 100 μ l 2 M H₂O₄ (Merck). The optical density (OD) was measured at A₄₅₀ nm using a plate reader (Biotek, Synergy 2, Winooski, Vermont, USA).

The results were analyzed with a parallel line assay in Microsoft Office Excel⁴⁵. We assessed the potency of the glycoforms relative to a standard, an independently titrated unmodified IgG1; these values were expressed as percentages relative to the unmodified glycoform.

Complement mediated lysis. Fifty μ l of washed, packed, D+ RBCs obtained from heparinized blood were mixed with 350 μ l 0.313 mM TNBS in 0.15 M Na₂HPO₄, pH 8.8 and incubated for 10 min at RT. TNPylated RBCs were centrifuged for 2 min at 350g and washed two times with PBS. RBC were resuspended into VBG+/+ (VB+/+ + 0.05 % w/v gelatin (Sigma-Aldrich)). Anti-TNP IgG1 was serially diluted in VBG-/- (3 mM Barbitol, 1.8 mM Sodium-Barbitol, 0.146 M NaCl, pH 7.4, 0.05 % w/v gelatin). In round bottom plates to a final volume of 100 μ l we combined the diluted IgG1, 10% serum, $\sim 4.5 \times 10^6$ RBC, and a glass bead (2 mm, Merck) to ensure mixing of the solution during incubation (1:1 final ratio VBG-/-:VBG+/+). This amount of RBC was taken to ensure the 100% absorbance between 1.8 and 2.2 delta (Δ) A412-A690 nm. The plates were incubated for 90 min at 37 °C while shaking at 150 rpm (Orbital incubator S150, 16 mm shaking diameter). After incubation, 1.25% w/v saponine was supplemented to the 100% control wells, 100 μ l VBG-/- was added to all wells and the plates were centrifuged for 2 min at 350 g. Subsequently, 150 μ l of supernatant was transferred into a separate plate and OD was measured at Δ A412-A690 nm using a plate reader. The percentage of lysed cells was calculated as follows:

$$\text{Lysis (\%)} = \frac{(\text{OD sample} - \text{OD spontaneous})}{(\text{OD 100\%} - \text{OD spontaneous})} \times 100$$

In GraphPad Prism we calculated the half maximal effective concentration (EC₅₀) for each replicate of the different glycoforms using a non-linear fit for normalized response with a variable slope and combined these to an average EC₅₀.

Statistical analysis. Statistical analyses were performed using GraphPad Prism version 6.00 for Windows (GraphPad Software, La Jolla, CA). The level of significance was set at p<0.05 using two-tailed tests.

Results

Recapitulation of all 20 major different glycoforms found in human plasma

Human IgG1, produced in human embryonic kidney (HEK) cells, shows complex-type biantennary glycans similar to IgG from normal human plasma (**Fig. 1a**)^{31,46}. More specifically, without any modification (“Unmodified”, box labelled “U” in the X-axis

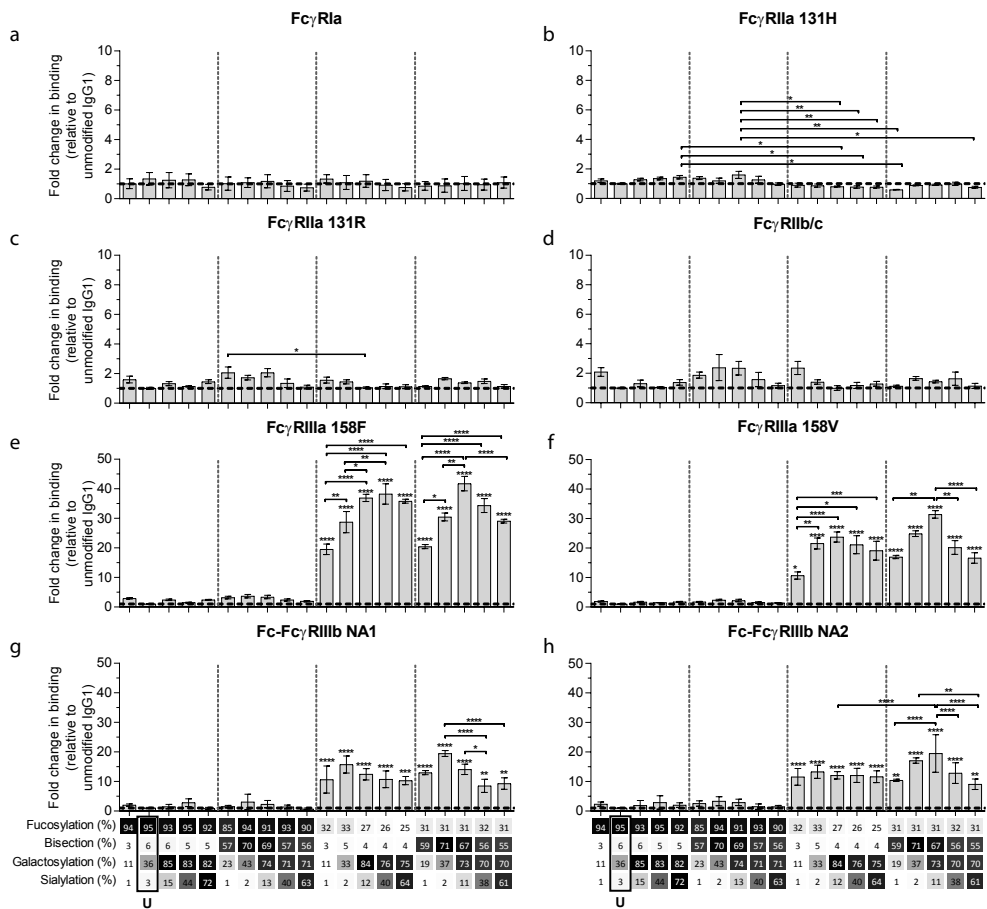


Figure 2. Binding of IgG glycoforms to human Fc γ R

Binding of IgG glycoforms to the human Fc γ R family as determined by SPR, displayed as relative binding compared to unmodified IgG1 (U), **a**) Fc γ R1, **b**) Fc γ R11a 131H, **c**) Fc γ R11a 131R, **d**) Fc γ R11b/c, **e**) Fc γ R11a V158, **f**) Fc γ R11a F158, **g**) Fc γ R11b NA1, and **h**) Fc γ R11b NA2. X-axis legend describes the percentage of each derived glycan trait indicated and by greyscale, from light to dark. The data represents the mean and SEM of at least 2 combined independent experiments; *, **, *** and **** (above each column as tested against unmodified, or as indicated, for Fc γ R11s comparing each set of five glycoforms defined by the vertical dotted lines, based on fucose and bisection levels) denote a statistical significance of $p \leq 0.05$, $p \leq 0.01$, $p \leq 0.001$ and $p \leq 0.0001$, respectively, as tested by one-way ANOVA using Tukey’s multiple comparisons test. U: Unmodified glycoform.

legend, **Fig. 1b-e**) HEK-derived IgG1 N-glycans feature high fucosylation, low bisection, intermediate-level galactosylation, and low sialylation (**Fig.1b-e**). We previously developed six glyco-engineering tools which can be implemented upon protein production, as we recently described³¹. These were aimed to decrease fucosylation, increase bisection, decrease or increase galactosylation, or increase sialylation. In the present study these tools were combined and used in all possible combinations during the transient transfection

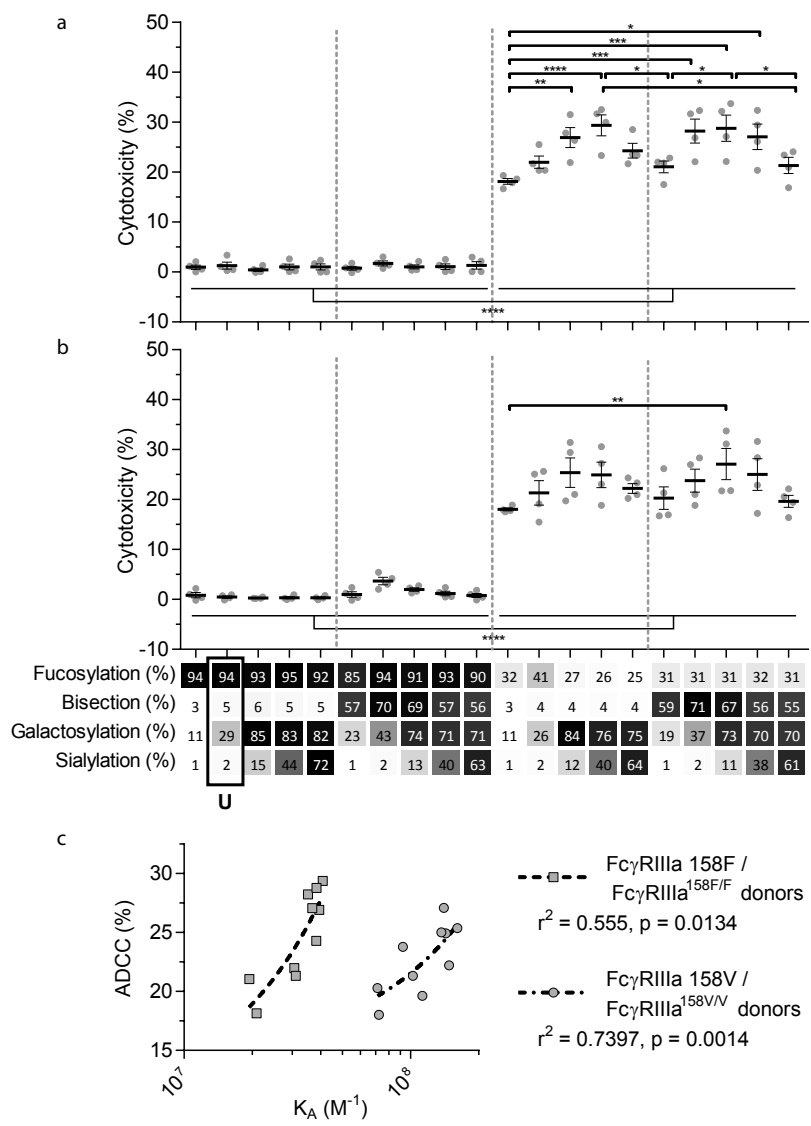


Figure 3. NK cell mediated ADCC of anti-D glycoform opsonized RBC
 ADCC mediated by NK cells from monozygotic Fc γ RIIIA^{158F/F} donors **(a)**, or monozygotic Fc γ RIIIA^{158V/V} donors **(b)**, data represents the mean and SEM of 4 combined independent experiments; *, **, *** and **** denote a statistical significance of $p \leq 0.05$, $p \leq 0.01$, $p \leq 0.001$ and $p \leq 0.0001$, respectively, as tested by one-way ANOVA using Tukey's multiple comparisons test. X-axis legend describes the percentage of each derived glycan trait indicated and by greyscale, from light to dark. **c**) Correlation between K_A of Fc γ RIIIa F158 or Fc γ RIIIa V158 binding of hypo-fucosylated glycoforms and ADCC activity of Fc γ RIIIA^{158F/F} or Fc γ RIIIA^{158V/V} donors respectively. r^2 and P value shown where obtained using a two-tailed Pearson's correlation. U: Unmodified glycoform.

in HEK cells, which resulted in the anticipated glycosylation changes and allowed us to produce the 20 major glycoforms present in human serum. Only minor unanticipated effects (**Fig. 1b-e**), were observed. A slight increase in galactosylation upon overexpression of beta 1,4-N-acetylglucosaminyltransferase III (GntIII) to increase bisection (E.g. 28 to 36% upon GntIII expression) – but this was only observed in samples with low starting-levels of galactosylation (**Fig. 1c-d**). Some of the tools caused a minor increase (<21%) in high-mannose or hybrid glycan species (**Supplementary Fig. 1, supplementary Table 1**)³¹. Using the glyco-engineering tools the most extreme levels were reached for fucose and galactose (**Fig. 1b, d**), bisection was increased up to 60%, and sialylation never reached over half of what was possible by the underlying galactose (~40%). The level of sialylation was therefore further increased using *in vitro* sialylation as described before (up to ~70%) (**Fig. 1e, Table 1**)^{31,47,48}. All in all, this resulted in 20 combinations and markedly different glycoforms. All 20 glycoforms were produced as two panels of IgG1, specific for the RhD (anti-D) antigen or 2,4,6-trinitrophenyl hapten (anti-TNP)³⁴, with both panels showing highly comparable glycosylation patterns depending of the glyco-engineering tools applied (**Table 1, supplementary Table 1**). To avoid any possible confounding effects of Fab glycosylation on IgG function, we used anti-D and anti-TNP with variable domains sequences devoid of N-linked glycosylation sites.

Binding of IgG glycome to human FcγR

We next used the IBIS MX96 biosensor system, as described in Dekkers et al.³⁹, capable of analyzing the binding of up to 48 different receptor ligand interactions in parallel by surface plasmon resonance (SPR), to probe the affinity of all IgG1-glycoforms to all human FcγRs and their allotypes affecting IgG binding (**Supplementary Table 2**)⁴⁹. The antibodies used for these experiments (anti-D) showed no signs of dimers or multimers (**Supplementary Fig. 2**). The binding affinities of unmodified IgG1 to the different receptors resembled those reported earlier (**Table 2**)⁴⁹. We considered significant changes in the apparent K_D of more than two fold from unmodified IgG to be potentially meaningful changes and within the scope of the SPR method, using a simplified 1:1 langmuir model that does not fully represent the actual interaction which is more complicated³⁹. No significant effects of glycan changes above two fold were seen on the binding to FcγRIa, FcγRIIa (neither the H131- or the R131-allotype) or FcγRIIb/c (**Fig. 2a-d**). However, marked changes were seen for all FcγRIII-isoforms. Reduction of fucose resulted in enhanced binding to all FcγRIII species by approximately 10-20-fold depending on the type- and allotype (**Fig. 2e-h**), as reported^{4,5}. Importantly, addition of galactose consistently enhanced binding of hypo-fucosylated IgG1 for all FcγRIIIa allotypes, doubling the effect of hypo-fucosylation alone (**Fig. 2e-f**). This effect was also seen for allotypes of FcγRIIIb, but less strong and only for IgG1 that was bisected in addition to hypo-fucosylated (**Fig. 2g-h**). Further sialylation of low-fucosylated galactosylated IgG1 had little additional effect on the binding to FcγRIII,

Table 2. Affinity of unmodified IgG1 (U) to the different FcγRs.Affinity in K_D as measured by SPR.

	Mean affinity	S.E.M.
FcγRI	3.0×10^{-9}	$\pm 8.7 \times 10^{-10}$
FcγRIIIa^{131H}	3.8×10^{-7}	$\pm 1.3 \times 10^{-8}$
FcγRIIIa^{131R}	4.8×10^{-7}	$\pm 2.8 \times 10^{-8}$
FcγRIIb	2.7×10^{-6}	$\pm 1.1 \times 10^{-7}$
FcγRIIIa^{158F}	1.3×10^{-6}	$\pm 9.5 \times 10^{-8}$
FcγRIIIa^{158V}	2.4×10^{-7}	$\pm 1.0 \times 10^{-8}$
FcγRIIIb NA1	3.2×10^{-6}	$\pm 4.7 \times 10^{-7}$
FcγRIIIb NA2	2.8×10^{-6}	$\pm 1.0 \times 10^{-7}$

except for hypo-fucosylated and bisected IgG1 for both allotypes of FcγRIIIa and FcγRIIIb NA2, where sialylation cause a significant decrease in binding. Taken together, glycan changes in the IgG-Fc only affect binding to FcγRIIIa and FcγRIIIb, with a major effect of hypo-fucosylation increasing binding to FcγRIIIa/b that was boosted by galactosylation. Bisection only appeared to indirectly affect binding when occurring in conjunction with sialylation, causing a slight decreased binding to FcγRIIIa/b to otherwise hypo-fucosylated and galactosylated IgG.

FcγRIIIa-mediated ADCC is steered by fucosylation and galactosylation

We next tested the efficacy of these anti-D IgG1 antibodies to mediate ADCC against RBC. Curiously, no NK cell-mediated induction of ADCC was seen with any fucosylated IgG1 at any concentration tested (**Fig. 3a, b** and **Supplementary Fig. 3**). Only hypo-fucosylated IgG1 induced ADCC in variable degrees depending on the glycosylation (**Fig. 3a, b**). The observed level of ADCC where in line with the binding results obtained by SPR for each of the FcγRIIIa allotypes (**Fig. 3c**), confirming the essential role of both hypo-fucosylation and elevated galactosylation for increased FcγRIIIa-binding and effector functions. Again, sialic acid had a minor but significant negative effect, especially for the bisected, hypo-fucosylated and galactosylated IgG1 (**Fig. 3a, b**). Remarkably, the well-known allotypic differences in affinity were confirmed by our SPR experiments, but not by the functional NK cell mediated ADCC.

Galactosylation and sialylation direct complement binding and activation

We then tested the effect of IgG-Fc glycosylation on C1q binding and subsequent

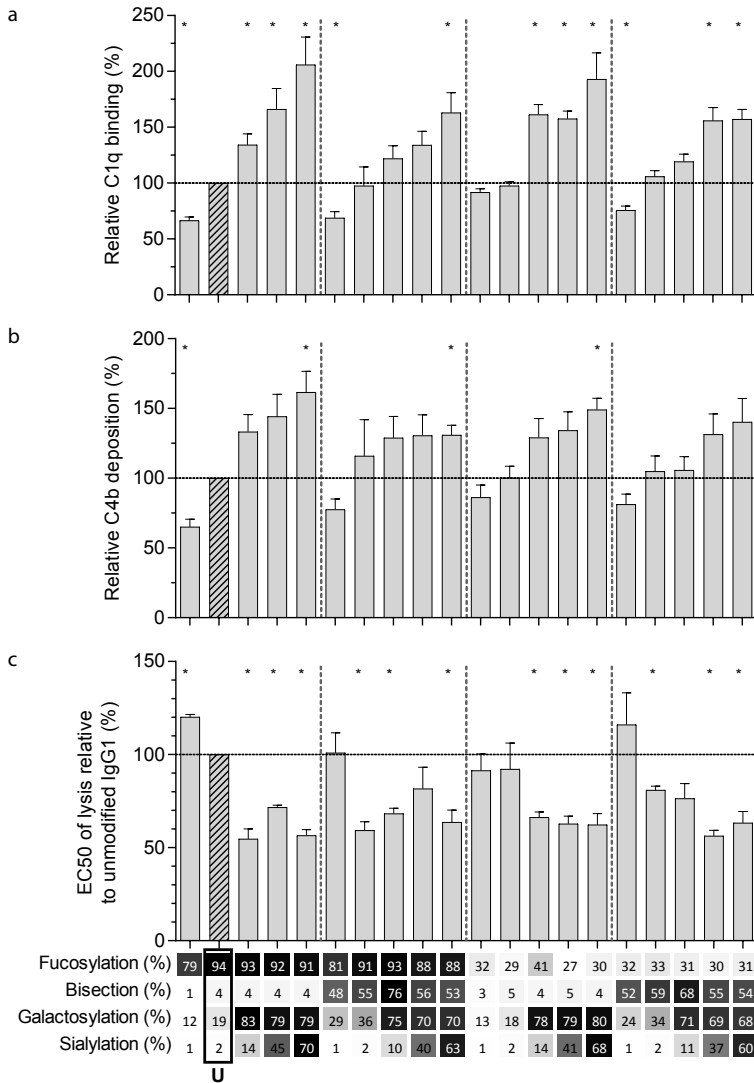


Figure 4. Complement activation by glyco-engineered anti-TNP IgG1

Relative **a**) binding of C1q (n=4) and **b**) C4 deposition as determined by ELISA (n=4), **c**) complement-mediated lysis of aTNP opsonized red blood cells (n=3). Data represents the mean and SEM of combined independent experiments; *denotes a statistical significance of $p \leq 0.05$, as tested by a one-sample t-test against a theoretical mean of 100 (%). X-axis legend describes the percentage of each derived glycan trait indicated and by greyscale, from light to dark. U: Unmodified glycoform.

complement activation, using the anti-TNP panel of IgG1 antibodies as anti-D does not fix complement. The efficiency of C1q binding to TNP-lated human serum albumin (TNP-HSA) and subsequent C4b deposition was titrated by serial dilution (**Supplementary Fig. 4**). All glycovariants of anti-TNP bound TNP-HSA equally well (**Supplementary Fig. 4a**),

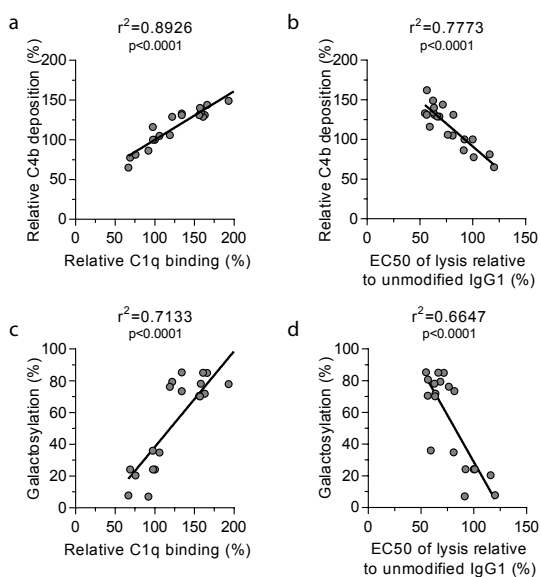


Figure 5. Correlations between complement activation and galactosylation

Correlation between **a)** C1q binding and C4 deposition, **b)** C4 deposition and complement mediated RBC lysis, **c)** galactosylation and C1q binding, and **d)** galactosylation and lysis, statistically tested using a two-tailed Pearson's correlation.

but C1q binding and C4b deposition differed profoundly for the different glycoforms (**Supplementary Fig. 4b**). The relative C1q binding and C4b deposition were then calculated (**Fig. 4a-b**, respectively). Both data sets suggested that elevated galactosylation and sialylation positively influenced complement activity. This activity was fully depended on the classical pathway with no influence of the mannan-binding lectin- or the alternative pathway, as C4b and C3b deposition, were completely blocked by an anti-C1q blocking antibody (**Supplementary Fig. 5**). We then determined if this also translates into more efficient complement-dependent cytotoxicity (CDC) by analyzing complement dependent lysis of TNP labeled RBC (**Fig. 4c, Supplementary Fig. 6**). The level of C1q binding of each glycoform correlated well with the C4b deposition (**Fig. 5a**) and with the obtained EC_{50} of CDC (**Fig. 5b**). The level of galactosylation of each glycoform also showed a direct relationship with the efficacy of C1q binding, and EC_{50} (**Fig. 5c, d**). In conclusion, the degree of galactosylation, but also sialylation of the IgG1-Fc N-glycan directly steers the antibody's efficacy to stimulate complement deposition and CDC.

Discussion

We have previously created an orthogonal set of glyco-engineering tools³¹ which we now combined to create 20 glycovariants of human IgG1, representing natural variants found in human plasma IgG, including extreme glycoforms found for examples in patients

with FNAIT and HDFN^{17,18,21,22}. These variants were investigated for their functional capacity to engage and activate FcγR and complement.

Of the FcγRs, we only observed an effect of glycosylation on binding to the FcγRIII-family of receptors, both FcγRIIIa and FcγRIIIb and their allotypes, which confirms and expands recent studies using a limited set of glycovariants presented here^{24,30}. Increased FcγRIII binding seems to be a general phenomenon for all IgG subclasses upon afucosylation^{50,51}. The positive binding effects were primarily caused by the lack of fucose, which was further strengthened by additional galactose. A similar effect has been observed for neutralizing anti-HIV antibody 2G12 produced in modified plant cells which showed better FcγRIIIa binding and antibody dependent (NK) cell-mediated viral inhibition⁵².

The enhanced binding of galactosylated and afucosylated IgG was slightly weakened by addition of sialic acid, but only if a bisecting GlcNAc was present. A similar negative effect of sialylation has previously been observed for mouse FcγR by Ravetch and colleagues⁵³. Importantly, we showed that the enhanced FcγRIII-binding effects are directly translated into increased FcγR-mediated cellular functions. We tested this using NK-cell mediated ADCC, as NK cells are the only cell type that only express FcγRIIIa. Curiously, we observed no ADCC at all for fucosylated IgG, even at high concentrations of IgG1. Thus, ADCC activity was only observed with afucosylated IgG1. Although somewhat surprising, this phenomenon has been observed previously for anti-Rhesus-mediated ADCC⁵⁴, but also for Rituximab-mediated B cell killing²⁷. This suggests that the enhanced affinity afucosylation of IgG has on FcγRIIIa binding is required to cross a signaling threshold of FcγRIIIa on NK cells required for killing.

The second surprise was that no significant difference was observed between ADCC-capacity of NK-cells from donors homozygous for one of the two FcγRIIIa-V/F158 allotypes, of which the V158 allele is known to have higher affinity for IgG (also confirmed here to be ~2-5x)⁴⁹. *In vitro*, this has been found result in stronger functional efficacy for the V158-variant⁵⁵⁻⁵⁷. *In vivo*, conflicting reports have showed that individuals homozygous either the V158 or the F158 allotype show stronger cellular clearance⁵⁸⁻⁶¹. It should be noted that most of these studies were performed before the knowledge of FcγRIII gene being influenced by copy number variation⁶¹. We also now know that NK cells can also express FcγRIIc or FcγRIIb in some individuals. Both these variations affect the functionality of this receptor^{32,62,63}. In this study we eliminated both these variables by selecting donors with two copies of FcγRIIIa and without FcγRIIc-ORF, possibly explaining these discrepancies, and perhaps suggesting that the 2-5 fold difference in affinity of IgG1 allotype is not enough to cause functional differences.

Importantly, the observed changes in FcγRIIIa-binding due to glycosylation reliably translated into functional NK-cell mediated ADCC lysis of RBC. For FcγRIIIa and FcγRIIIb it was known that absence of IgG-Fc core-fucosylation increases the affinity of interaction due to a glycan-glycan interaction between the Fc glycan and the N162-glycan uniquely

found in the FcγRIII family¹¹. Our approach to combine this with multiple end glycan editing shows an additional layer of complexity exerted by the galactose and sialic acid. The reasons for this added effect of galactose is unknown but may very well be related to the subtle effects on quaternary structure of the Fc-domain^{64,65} but may also be related to differential interaction of the Fc-glycan with the N162-glycan found in FcγRIII¹¹.

The possible effect of the Fc-glycans on complement activity, has until now remained enigmatic. It has been proposed for a long time that agalactosylated IgG activates complement more efficiently through the lectin pathway (MBL)²⁵. To our knowledge these results have never been confirmed. On the contrary, we saw enhanced complement activity of all glycovariants with elevated galactose, and no evidence of MBL being activated by any of our glycoforms. These results confirm recent work also suggesting galactosylation of IgG1 to positively influence C1q binding and CDC^{26,66}. In addition, our results clearly rule out fucosylation or bisection having an effect on complement activation, and we now show that sialylation increases the C1q-binding of galactosylated IgG. This effect of sialylation was observed on all different glycan backbones (e.g. with or without fucose, with or without bisection) which is highly suggestive that this is no artefactual finding. This is in contrast with the previously mentioned study showing that additional sialylation decreases C1q binding²⁶. Activation of complement is dependent on spatial arrangement of the IgG on the cell surface⁶⁷ which is likely to differ considerably between each monoclonal antibody and target, and may possibly explain the discrepancies found between our two studies. This view is supported by our observations that sialylation had limited if any effect on IgG-mediated CDC using RBC as targets, while binding to C1q of anti-TNP antibodies was enhanced by sialylated IgG-on solid surfaces.

Low galactosylation level in total IgG generally correlates with disease severity of several autoimmune diseases, such as rheumatoid arthritis and multiple sclerosis^{13,14}. While this may seem at odds with our observations at first glance, with high galactosylated IgG having elevated complement and FcγR activities, both notions are in agreement if the balance between total- and antigen-specific glycosylation is taken into account. In this way, low potential for FcγR- and C1q binding for total IgG (e.g. low galactosylation), creates a pro-inflammatory environment in which clinical manifestations can take hold as this lowers the threshold for pathogenic antibodies. Antigen-specific IgG can also potentially have different glycosylation features than total IgG as we have shown before^{17,18,21,22}, and if these are more pro-inflammatory than that of total IgG, this can theoretically lead to enhanced immune activation and clinical symptoms. The knowledge obtained in the current research provides a roadmap to decipher the meaning of glycan profiles in these diseases settings.

In summary, we show here that a set of glyco-engineering techniques we recently developed³¹ can be combined to quickly generate any desired IgG glycoforms to test the effect on functional capacity. Using two sets of monoclonal antibodies we generated the most extreme 20 different glycoforms possible, and examined their effect on binding to

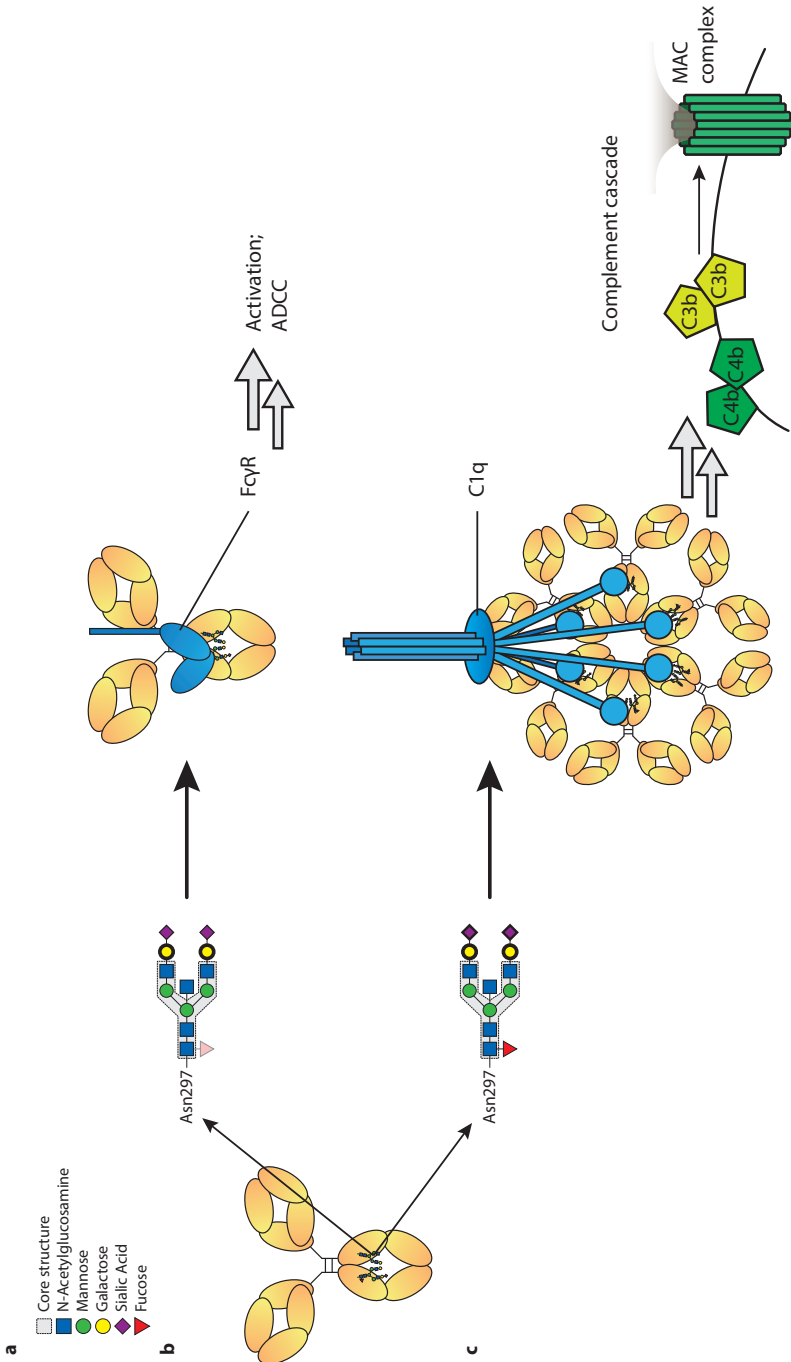


Figure 6. Proposed model of influence of IgG-Fc glycan composition on effector functions

a) Standard composition of bi-antennary Fc-glycan. **b)** Afucosylation of IgG Fc glycan increases binding affinity to FcγRIII and subsequent antibody-mediated functions, such as antibody dependent cellular cytotoxicity (ADCC). In addition galactosylation further increases affinity to FcγRIII and function of afucosylated IgG. **c)** Galactosylation enhances binding of IgG to complement component C1q and activation of the classical complement pathway, which results in cleavage of complements C4, C3, and further initiation of the membrane attack complex (MAC). Sialylation may further increase C1q binding and complement activation. Glycan residues that need to be present to enhance indicated effector function (ADCC/CDC) are displayed with bolder lines, and for those that need to be absent to enhance indicated effector functions are displayed with faded colors.

FcγR and complement, as well as their functional capacity to trigger cytotoxicity. These revealed firstly that the normal glycosylation changes seen in human IgG1 do not affect any other FcγR than FcγRIIIa and FcγRIIIb. Secondly, hypo-fucosylation and galactosylation increase binding to both human FcγRIII-variants, with a minor negative effect of sialic acid and bisecting GlcNAc. In addition, galactosylation is the primary glycan adduct that enhances C1q-binding and all downstream complement activities, including CDC. This is summarized in **Fig. 6**. Collectively, this indicates that afucosylated and hyper-galactosylated IgG1 antibodies have both improved ADCC and complement mediated activities, including complement opsonization and CDC. These properties can now be systematically implemented in new therapeutic antibodies for enhanced effector functions. Even as important, this also allows us to decipher the clinical potency of antibodies in immune responses that have tendency to have altered fucosylation and/or galactosylation^{17,18,21,22}.

Acknowledgements

The authors would like to thank Ninotska Derksen, Pleuni De Heer-Ooijevaar, Prof. Dr. Rob Aalberse and Sanne van de Bovenkamp for practical help, and, Prof. Dr. Ellen van der Schoot, Prof. Dr. Rob Aalberse, Sanne van de Bovenkamp, Dr. Juan J. Garcia-Vallejo, Willem Falkenburg and Christine Bruggeman for fruitful discussions, and Prof. Dr. Ellen van der Schoot for critically reading the manuscript.

This study was supported by Sanquin Product and Process Development Plasma Products, 12-001.

Author contributions

GD, TK, DW, TR, MW and GV designed the research. GD, AB, DW, TR, MW and GV designed the experiments. GD, LT, RP, AB, MB, CK, SL, RV and YM performed the experiments. GD, RP, AB, MB, CK, TR, TK, MW, and GV analyzed data, GD and GV wrote the manuscript. All authors contributed to and approved the final manuscript.

Conflicts of Interest disclosure

The authors declare no conflict of interest.

References

1. Bruhns, P. & Jönsson, F. Mouse and human FcR effector functions. *Immunol. Rev.* 268, 25–51 (2015).
2. Weiner, L. M., Surana, R. & Wang, S. Monoclonal antibodies: versatile platforms for cancer immunotherapy. *Nat. Rev. Immunol.* 10, 317–327 (2010).
3. Weiner, G. J. Building better monoclonal antibody-based therapeutics. *Nat. Rev. Cancer* 15, 361–70 (2015).
4. Shields, R. L. et al. Lack of fucose on human IgG1 N-linked oligosaccharide improves binding to human Fcγ₃RIII and antibody-dependent cellular toxicity. *J. Biol. Chem.* 277, 26733–40 (2002).
5. Shinkawa, T. et al. The absence of fucose but not the presence of galactose or bisecting N-acetylglucosamine of human IgG1 complex-type oligosaccharides shows the critical role of enhancing antibody-dependent cellular cytotoxicity. *J. Biol. Chem.* 278, 3466–73 (2003).
6. Beck, A. & Reichert, J. M. Marketing approval of mogamulizumab: A triumph for glyco-engineering. *mAbs* 4, 419–425 (2012).
7. Subedi, G. P., Hanson, Q. M. & Barb, A. W. Restricted motion of the conserved immunoglobulin G1 N-glycan is essential for efficient Fcγ₃RIIIa binding. *Structure* 22, 1478–88 (2014).
8. Jefferis, R. Recombinant antibody therapeutics: the impact of glycosylation on mechanisms of action. *Trends Pharmacol. Sci.* 30, 356–62 (2009).
9. Caaveiro, J. M. M., Kiyoshi, M. & Tsumoto, K. Structural analysis of Fc/Fcγ₃R complexes: a blueprint for antibody design. *Immunol. Rev.* 268, 201–221 (2015).
10. Sondermann, P., Huber, R., Oosthuizen, V. & Jacob, U. The 3.2-Å crystal structure of the human IgG1 Fc fragment-Fc γ₃RIII complex. *Nature* 406, 267–73 (2000).
11. Ferrara, C. et al. Unique carbohydrate-carbohydrate interactions are required for high affinity binding between Fcγ₃RIII and antibodies lacking core fucose. *Proc. Natl. Acad. Sci. U. S. A.* 108, 12669–74 (2011).
12. Baković, M. P. et al. High-throughput IgG Fc N-glycosylation profiling by mass spectrometry of glycopeptides. *J. Proteome Res.* 12, 821–31 (2013).
13. Bondt, A. et al. Association between galactosylation of immunoglobulin G and improvement of rheumatoid arthritis during pregnancy is independent of sialylation. *J. Proteome Res.* 12, 4522–31 (2013).
14. Wuhrer, M. et al. Pro-inflammatory pattern of IgG1 Fc glycosylation in multiple sclerosis cerebrospinal fluid. *J. Neuroinflammation* 12, 235 (2015).
15. Chen, G. et al. Human IgG Fc-glycosylation profiling reveals associations with age, sex, female sex hormones and thyroid cancer. *J. Proteomics* 75, 2824–34 (2012).
16. Wuhrer, M. et al. Regulated glycosylation patterns of IgG during alloimmune responses against human platelet antigens. *J. Proteome Res.* 8, 450–6 (2009).
17. Kapur, R. et al. Low anti-RhD IgG-Fc-fucosylation in pregnancy: a new variable predicting severity in haemolytic disease of the fetus and newborn. *Br. J. Haematol.* 166, 936–45 (2014).
18. Sonneveld, M. E. et al. Glycosylation pattern of anti-platelet IgG is stable during pregnancy and predicts clinical outcome in alloimmune thrombocytopenia. *Br. J. Haematol.* 174, 310–20 (2016).
19. Ackerman, M. E. et al. Natural variation in Fc glycosylation of HIV-specific antibodies impacts antiviral activity. *J. Clin. Invest.* 123, 2183–92 (2013).
20. Wang, T. T. et al. IgG antibodies to dengue enhanced for Fcγ₃RIIIA binding determine disease

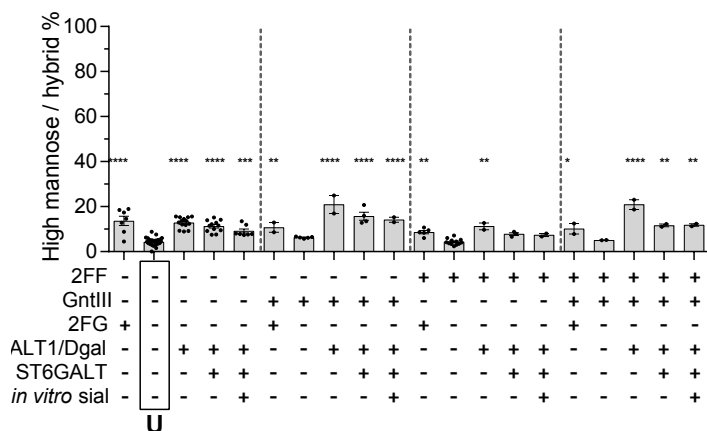
- severity. *Science* 355, 395–398 (2017).
21. Kapur, R. et al. A prominent lack of IgG1-Fc fucosylation of platelet alloantibodies in pregnancy. *Blood* 123, 471–80 (2014).
 22. Sonneveld, M. E. et al. Antigen specificity determines anti-red blood cell IgG-Fc alloantibody glycosylation and thereby severity of haemolytic disease of the fetus and newborn. *Br. J. Haematol.* 176, 651–660 (2017).
 23. Kapur, R. et al. C-reactive protein enhances IgG-mediated phagocyte responses and thrombocytopenia. *Blood* 125, 1793–802 (2015).
 24. Thomann, M. et al. In vitro glycoengineering of IgG1 and its effect on Fc receptor binding and ADCC activity. *PLoS One* 10, e0134949 (2015).
 25. Malhotra, R. et al. Glycosylation changes of IgG associated with rheumatoid arthritis can activate complement via the mannose-binding protein. *Nat. Med.* 1, 237–43 (1995).
 26. Quast, I. et al. Sialylation of IgG Fc domain impairs complement-dependent cytotoxicity. *J. Clin. Invest.* 125, 4160–4170 (2015).
 27. Li, H. et al. Optimization of humanized IgGs in glycoengineered *Pichia pastoris*. *Nat. Biotechnol.* 24, 210–5 (2006).
 28. Yang, Z. et al. Engineered CHO cells for production of diverse, homogeneous glycoproteins. *Nat. Biotechnol.* 33, 2014–2017 (2015).
 29. Meuris, L. et al. GlycoDelete engineering of mammalian cells simplifies N-glycosylation of recombinant proteins. *Nat. Biotechnol.* 32, 485–9 (2014).
 30. Subedi, G. P. & Barb, A. W. The immunoglobulin G1 N-glycan composition affects binding to each low affinity Fc γ receptor. *MAbs* 8, 1512–1524 (2016).
 31. Dekkers, G. et al. Multi-level glyco-engineering techniques to generate IgG with defined Fc-glycans. *Sci. Rep.* 6, 36964 (2016).
 32. van der Heijden, J. et al. Phenotypic variation in IgG receptors by nonclassical FCGR2C alleles. *J. Immunol.* 188, 1318–24 (2012).
 33. Della Valle, L. et al. The majority of human memory B cells recognizing RhD and tetanus resides in IgM+ B cells. *J. Immunol.* 193, 1071–9 (2014).
 34. Kruijsen, D. et al. Intranasal administration of antibody-bound respiratory syncytial virus particles efficiently primes virus-specific immune responses in mice. *J. Virol.* 87, 7550–7 (2013).
 35. Chambers, M. C. et al. A cross-platform toolkit for mass spectrometry and proteomics. *Nat. Biotechnol.* 30, 918–20 (2012).
 36. Plomp, R. et al. Hinge-Region O-Glycosylation of Human Immunoglobulin G3 (IgG3). *Mol. Cell. Proteomics* 14, 1373–84 (2015).
 37. Ory, P. A., Clark, M. R., Kwoh, E. E., Clarkson, S. B. & Goldstein, I. M. Sequences of complementary DNAs that encode the NA1 and NA2 forms of Fc receptor III on human neutrophils. *J. Clin. Invest.* 84, 1688–91 (1989).
 38. Rodenko, B. et al. Generation of peptide-MHC class I complexes through UV-mediated ligand exchange. *Nat. Protoc.* 1, 1120–32 (2006).
 39. Dekkers, G. et al. Affinity of human IgG subclasses to mouse Fc gamma receptors. *MAbs* 9, 767–773 (2017).
 40. de Lau, W. et al. Lgr5 homologues associate with Wnt receptors and mediate R-spondin signalling. *Nature* 476, 293–7 (2011).
 41. Schasfoort, R. B. M. et al. Interpolation method for accurate affinity ranking of arrayed ligand-analyte interactions. *Anal. Biochem.* 500, 21–3 (2016).

42. McGrath, F. D. G. et al. Evidence that complement protein C1q interacts with C-reactive protein through its globular head region. *J. Immunol.* 176, 2950–7 (2006).
43. Leito, J. T. D., Ligtenberg, A. J. M., van Houdt, M., van den Berg, T. K. & Wouters, D. The bacteria binding glycoprotein salivary agglutinin (SAG/gp340) activates complement via the lectin pathway. *Mol. Immunol.* 49, 185–90 (2011).
44. Hack, C. E. et al. Disruption of the internal thioester bond in the third component of complement (C3) results in the exposure of neodeterminants also present on activation products of C3. An analysis with monoclonal antibodies. *J. Immunol.* 141, 1602–9 (1988).
45. Armitage, P. & Colton, T. *Encyclopedia of Biostatistics.* (John Wiley & Sons, Ltd, 2005). doi:10.1002/0470011815
46. Fokkink, W. J. R. et al. Comparison of Fc N-Glycosylation of Pharmaceutical Products of Intravenous Immunoglobulin G. *PLoS One* 10, e0139828 (2015).
47. Barb, A. W., Brady, E. K. & Prestegard, J. H. Branch-specific sialylation of IgG-Fc glycans by ST6Gal-I. *Biochemistry* 48, 9705–7 (2009).
48. Washburn, N. et al. Controlled tetra-Fc sialylation of IVIg results in a drug candidate with consistent enhanced anti-inflammatory activity. *Proc. Natl. Acad. Sci. U. S. A.* 112, 201422481 (2015).
49. Bruhns, P. et al. Specificity and affinity of human Fcγ receptors and their polymorphic variants for human IgG subclasses. *Blood* 113, 3716–25 (2009).
50. Niwa, R. et al. IgG subclass-independent improvement of antibody-dependent cellular cytotoxicity by fucose removal from Asn297-linked oligosaccharides. *J. Immunol. Methods* 306, 151–60 (2005).
51. Bruggeman, C. W. et al. Enhanced Effector Functions Due to Antibody Defucosylation Depend on the Effector Cell Fcγ Receptor Profile. *J. Immunol.* 199, 204–211 (2017).
52. Forthal, D. N. et al. Fc-glycosylation influences Fcγ receptor binding and cell-mediated anti-HIV activity of monoclonal antibody 2G12. *J. Immunol.* 185, 6876–82 (2010).
53. Kaneko, Y., Nimmerjahn, F. & Ravetch, J. V. Anti-inflammatory activity of immunoglobulin G resulting from Fc sialylation. *Science* 313, 670–3 (2006).
54. Sibérl, S. et al. Selection of a human anti-RhD monoclonal antibody for therapeutic use: impact of IgG glycosylation on activating and inhibitory Fc gamma R functions. *Clin. Immunol.* 118, 170–9 (2006).
55. López-Albaitero, A. et al. Role of polymorphic Fc gamma receptor IIIa and EGFR expression level in cetuximab mediated, NK cell dependent in vitro cytotoxicity of head and neck squamous cell carcinoma cells. *Cancer Immunol. Immunother.* 58, 1853–64 (2009).
56. Hatjiharissi, E. et al. Increased natural killer cell expression of CD16, augmented binding and ADCC activity to rituximab among individuals expressing the Fc{gamma}RIIIa-158 V/V and V/F polymorphism. *Blood* 110, 2561–4 (2007).
57. Oboshi, W. et al. The influence of NK cell-mediated ADCC: Structure and expression of the CD16 molecule differ among FcγRIIIa-V158F genotypes in healthy Japanese subjects. *Hum. Immunol.* 77, 165–71 (2016).
58. Stegmann, T. C. et al. Rhlg-prophylaxis is not influenced by FCGR2/3 polymorphisms involved in red blood cell clearance. *Blood* 129, 1045–1048 (2017).
59. Cartron, G. et al. Therapeutic activity of humanized anti-CD20 monoclonal antibody and polymorphism in IgG Fc receptor FcγRIIIa gene. *Blood* 99, 754–8 (2002).
60. Burkhardt, B. et al. Impact of Fc gamma-receptor polymorphisms on the response to rituximab treatment in children and adolescents with mature B cell lymphoma/leukemia. *Ann. Hematol.*

95, 1503–12 (2016).

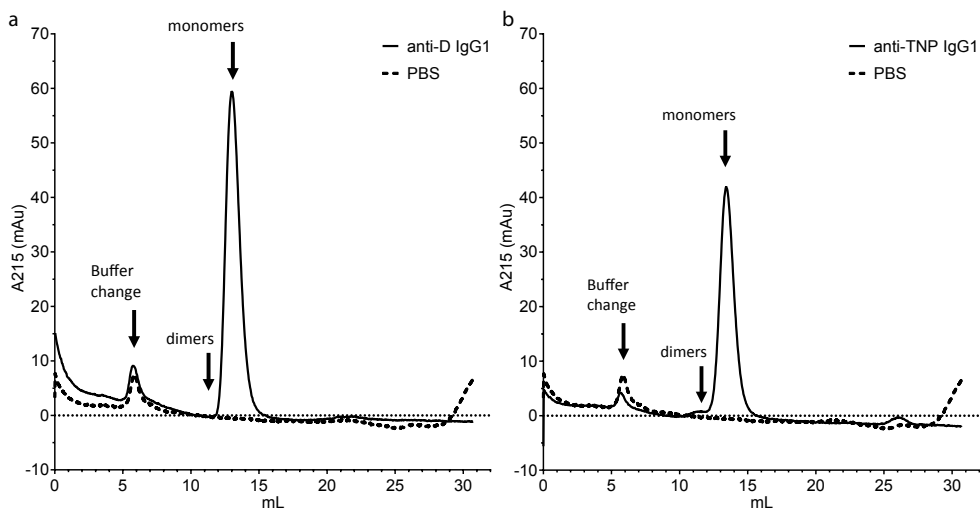
61. Kumpel, B. M., De Haas, M., Koene, H. R., Van De Winkel, J. G. J. & Goodrick, M. J. Clearance of red cells by monoclonal IgG3 anti-D in vivo is affected by the VF polymorphism of Fcγ₃ (CD16). *Clin. Exp. Immunol.* 132, 81–6 (2003).
62. Aitman, T. J. et al. Copy number polymorphism in Fcγ₃ predisposes to glomerulonephritis in rats and humans. *Nature* 439, 851–5 (2006).
63. Thabet, M. M. et al. Contribution of Fcγ₃ receptor IIIA gene 158V/F polymorphism and copy number variation to the risk of ACPA-positive rheumatoid arthritis. *Ann. Rheum. Dis.* 68, 1775–80 (2009).
64. Ahmed, A. a et al. Structural characterization of anti-inflammatory immunoglobulin G Fc proteins. *J. Mol. Biol.* 426, 3166–79 (2014).
65. Le, N. P. L., Bowden, T. A., Struwe, W. B. & Crispin, M. Immune recruitment or suppression by glycan engineering of endogenous and therapeutic antibodies. *Biochim. Biophys. Acta* 1860, 1655–68 (2016).
66. Pace, D. et al. Characterizing the effect of multiple Fc glycan attributes on the effector functions and Fcγ₃ receptor binding activity of an IgG1 antibody. *Biotechnol. Prog.* 1–12 (2016). doi:10.1002/btpr.2300
67. Diebold, C. a. et al. Complement is activated by IgG hexamers assembled at the cell surface. *Science* 343, 1260–3 (2014).

Supplementary



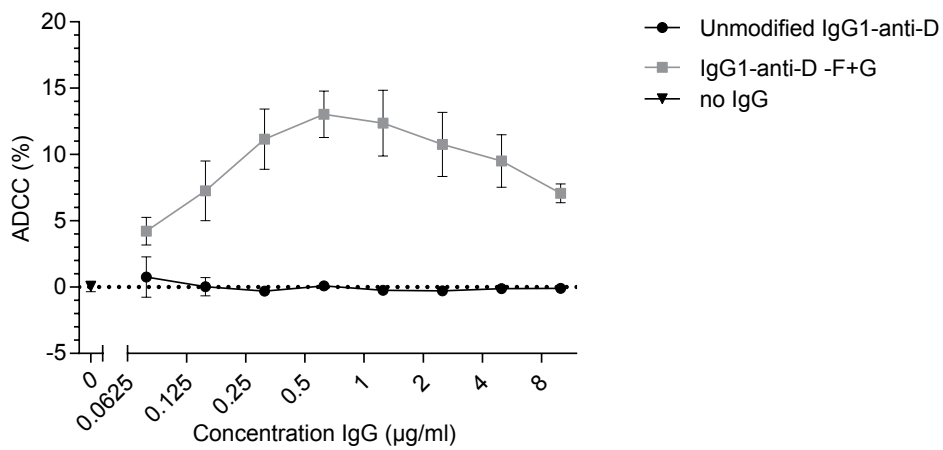
Supplementary figure 1. Hybrid-type and high-mannose glycosylation of glycoforms

Sum of Hybrid-type and high-mannose glycopeptide abundance in the 20 different glyco-engineered IgG1 glycoforms. Data represents the mean and SEM of independent experiments; *, **, *** and **** denote a statistical significance of $p < 0.05$, $p < 0.01$, $p < 0.001$ and $p < 0.0001$, respectively, as tested by one-way ANOVA against unmodified IgG1, using Dunnett's multiple comparisons test.



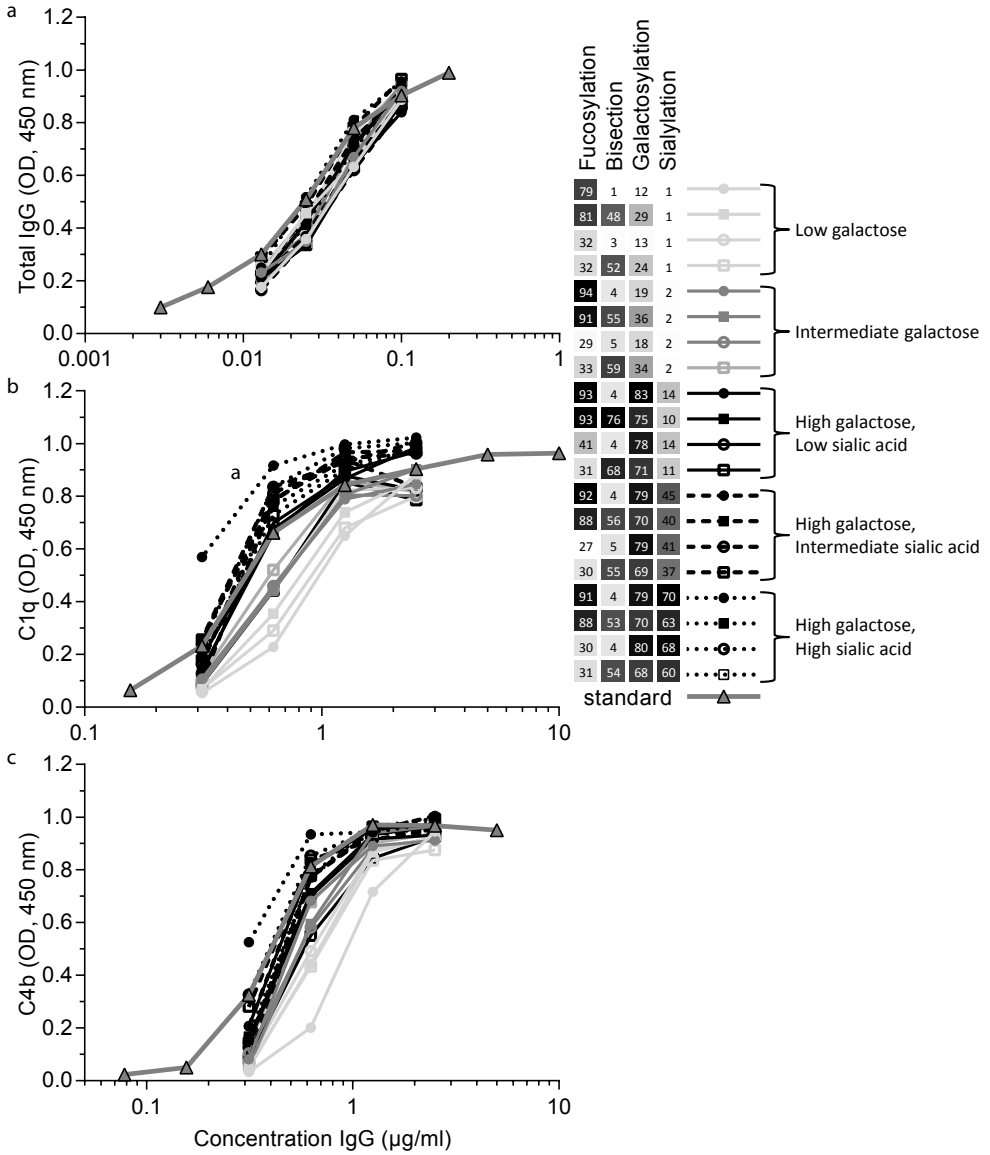
Supplementary figure 2. HPLC analysis of purified IgG1

Representative HP-SEC chromatograms of unmodified anti-D **(a)** or anti-TNP **(b)** IgG1 run on HPLC Superdex 200 10/300 gel filtration column, **(a)** shows for anti-D only a monomeric peak is observed and no dimeric peak, **(b)** shows for anti-TNP besides the large monomeric peak a small dimeric peak (<2% of total).



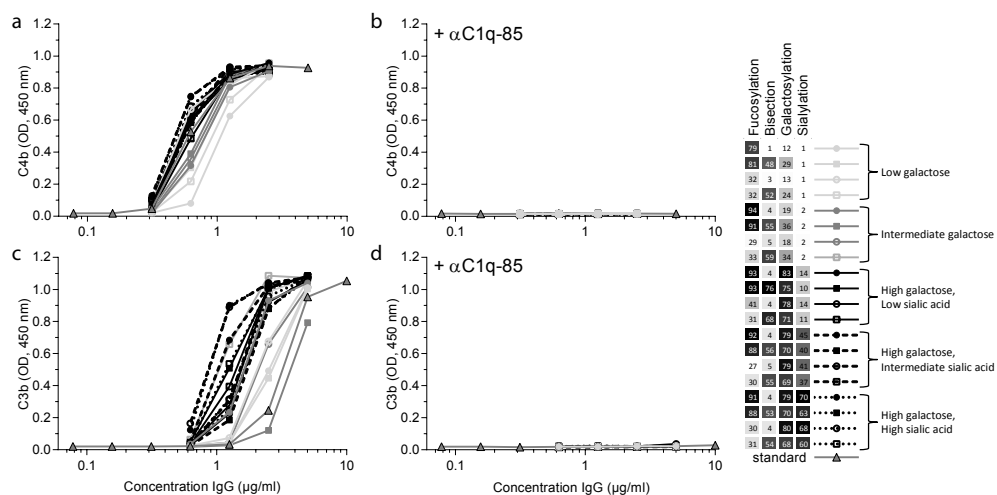
Supplementary Figure 3. Titration ADCC

Titration of IgG glycoforms in ADCC assay; data represents means and SD of two donors, (-F+G: hypofucosylated and hypergalactosylated IgG1).



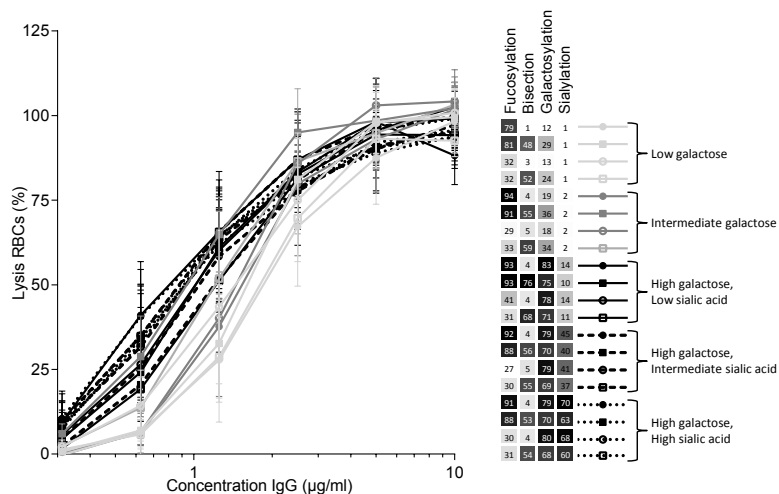
Supplementary Figure 4. IgG, C1q binding and C4b deposition as measured by ELISA

Raw data and control ELISA data of complement ELISA with HSA-TNP coat, followed by incubation with aTNP IgG1 glycoforms and subsequent complement deposition by incubation with human. **a)** anti-total human IgG, **b)** anti-C1q and **c)** anti-C4b detection respectively. Data are representative of n=6. As legend describes: the line color from light grey to black represents low to high galactosylation respectively, solid line to more dashed represents low to high sialylation respectively, open or filled symbols represent low or high fucose respectively and circle or square symbols represent low or high bisection respectively. From panels **b** and **c** we can conclude that all high galactosylated and sialylated are more active than low galactosylated and sialylated which are relatively more left or right of the standard curve respectively.



Supplementary Figure 5. C4b and C3b deposition requires C1q activity

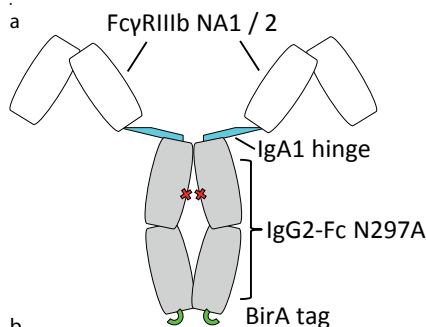
Complement ELISA with HSA-TNP coat, incubation with aTNP IgG1 glycoforms, subsequently incubation with pooled human serum, HRP-labeled-anti-C4b (**a, b**) or biotin-anti-C3b and subsequent strep-HRP (**c, d**), (**a, c**) control plates (**c, d**) incubated with anti-C1q-85 blocking antibody, data are representative of $n = 2$. As legend describes: the line color from light grey to black represents low to high galactosylation respectively, solid line to more dashed represents low to high sialylation respectively, open or filled symbols represent low or high fucose respectively and circle or square symbols represent low or high bisection respectively. No C4b or C3b deposition was detected with C1q blocking, both can respectively be found when the lectin or alternative pathway is activated, showing no involvement of either pathway.



Supplementary Figure 6. TNP labeled RBC incubated with anti-TNP IgG glycoforms and pooled human serum

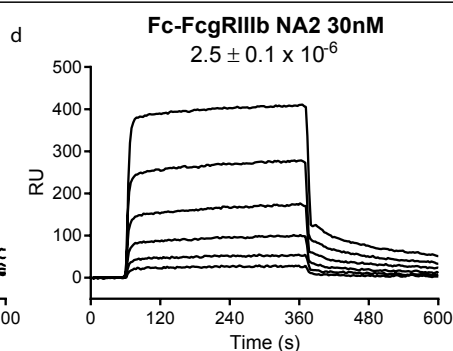
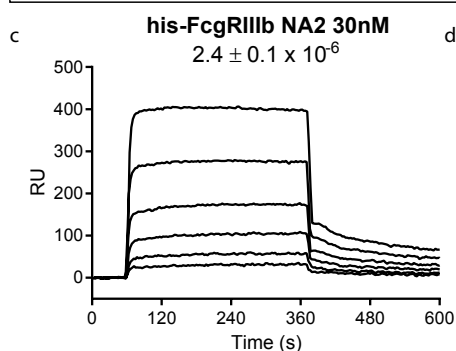
Lysis was measured as hemoglobin release into the supernatant by spectrophotometer ($OD_{450} - OD_{650}$) and calculated relative to signal of maximum lysis control (2.5% saponine). Data are means and SD of 2 representative experiments 3 in total, each carried out in duplo. As legend describes: the line color from light grey to black represents low to high galactosylation respectively, solid line to more dashed represents low to high sialylation respectively, open or filled symbols represent low or high fucose respectively

and circle or square symbols represent low or high bisection respectively. We can conclude that all high galactosylated and sialylated IgG1 are more active than low galactosylated and sialylated IgG1 which are relatively more left or right respectively.



b

Fc-FcγRIIIB_NA1	MWQLLLPTAL	LLLVSAGMRT	EDLPKAVVFL	EPQWYR	VLEK	DSVTLKCCQA	YSPEDNSTQW	60	
Fc-FcγRIIIB_NA2	MWQLLLPTAL	LLLVSAGMRT	EDLPKAVVFL	EPQWYS	VLEK	DSVTLKCCQA	YSPEDNSTQW	60	
Fc-FcγRIIIB_NA1	FHNENL	ASSYFIDAAT	V	DSGEYRCQ	TNLSTLSDPV	QLEVH	IGWLL	LQAPRWVFE	120
Fc-FcγRIIIB_NA2	FHNESL	ASSYFIDAAT	V	DSGEYRCQ	TNLSTLSDPV	QLEVH	IGWLL	LQAPRWVFE	120
Fc-FcγRIIIB_NA1	EDPIHLRCHS	WKNTALHKVT	YLQNGKDRKY	FHHNSDFHIP	KATLKDSGSY	FCRGLVGSKN		180	
Fc-FcγRIIIB_NA2	EDPIHLRCHS	WKNTALHKVT	YLQNGKDRKY	FHHNSDFHIP	KATLKDSGSY	FCRGLVGSKN		180	
Fc-FcγRIIIB_NA1	VSSETVNITI	TQEF	PVPSTP	PTPSPSTPPT	PSPSCCHAPP	VAGPSVFLFP	PKPKDTLMIS	240	
Fc-FcγRIIIB_NA2	VSSETVNITI	TQEF	PVPSTP	PTPSPSTPPT	PSPSCCHAPP	VAGPSVFLFP	PKPKDTLMIS	240	
Fc-FcγRIIIB_NA1	RTPEVTCVVV	DVSHEDPEVQ	FNWYVDGVEV	HNAKTKPREE	Q	FASTFRVVS	VLTVVHQDWL	300	
Fc-FcγRIIIB_NA2	RTPEVTCVVV	DVSHEDPEVQ	FNWYVDGVEV	HNAKTKPREE	Q	FASTFRVVS	VLTVVHQDWL	300	
Fc-FcγRIIIB_NA1	NGKEYCKKVS	NKGLPAPIEK	TISKTKGQPR	EPQVYTLPPS	REEMTKNQVS	LTCLVKGFYP		360	
Fc-FcγRIIIB_NA2	NGKEYCKKVS	NKGLPAPIEK	TISKTKGQPR	EPQVYTLPPS	REEMTKNQVS	LTCLVKGFYP		360	
Fc-FcγRIIIB_NA1	SDIAVEWESN	GQPENNYKTT	PPMLSDGSF	FLYSKLTVDK	SRWQQGNVFS	CSVMHEALHN		420	
Fc-FcγRIIIB_NA2	SDIAVEWESN	GQPENNYKTT	PPMLSDGSF	FLYSKLTVDK	SRWQQGNVFS	CSVMHEALHN		420	
Fc-FcγRIIIB_NA1	HYTQKSLSL	PGK	GLNDIFE	AQKIEW				446	
Fc-FcγRIIIB_NA2	HYTQKSLSL	PGK	GLNDIFE	AQKIEW				446	



Supplementary Figure 7. FcγRIIIB-Fc Fusion construct

Model **(a)** and amino acid sequence **(b)** of the FcγRIIIB_NA1_IgA1Hinge_IgG2-Fc_N297A_BirA-tag and FcγRIIIB_NA2_IgA1Hinge_IgG2-Fc_N297A_BirA-tag, shown in white; FcγR, yellow; NA1/NA2 differences, blue; IgA1 hinge, grey; IgG2Fc, red; N297A substitution, green; BirA-tag, **c, d**. SPR analysis on IBIS MX96 of binding of unmodified IgG to the his-tag captured FcγRIIIB NA2 **(c)** or in house produced FcγRIIIB_NA2-Fc fusion **(d)** shows comparable binding affinities in K_D and SD ($n = 3$).

Supplementary table 1. Comprehensive list of glycopeptide degrees of complex glycans found in the glyco-engineered IgG1 batches of anti-D and anti-TNP specificity

2FG (0.4 mM 2-deoxy-2-fluoro-L-fucose), 2FG (1 mM 2-deoxy-2-fluoro-D-galactose), GNT3 (co-transfection of 1% GNT3 vector), B4GALT1/D-galactose (co-transfection of 1% B4GALT1 vector and addition of 5 mM D-galactose), ST6GALT (co-transfection of 2.5% ST6GALT vector), and *in vitro* sialylation (treatment of sample with recombinant ST6GALT and CMP-NANA). These resulted in significantly different glycosylation traits (fucosylation, bisection, galactosylation, sialylation, high-mannose, hybrid-type), which are calculated from the relative abundances of individual N-glycans. The shading of cells indicates, for each glycoform the lowest to highest abundance of glycopeptides, respectively, from light to dark.

name	glyco-engineering		relative abundance glycopeptides*																								
	2FG (-)	GNT3 (+B)	B4GALT1/D-galactose (+G)	ST6GALT (+S)	<i>in vitro</i> sialylation (+vs)	H5N3F1	H6N3F1	H6N4F1	H6N5F1	H5N3F1S1	H6N4F1S1	H6N3F1S1	H5N3F1S1	H6N4S1	H6N5S1	H3N3F1	H3N3F1	H4N3F1S1	H3N3	H4N3	H4N3S1	H5N2	H6N2	H7N2	H8N2	H9N2	
anti-D																											
-G	-	-	-	-	-	0.5	0.1	0.7	0.0	0.1	0.2	0.0	0.1	0.1	0.0	0.0	0.0	0.0	0.0	0.0	0.0	0.0	0.0	0.0	0.0	0.0	0.0
Unmodified	-	-	-	-	-	0.2	0.1	0.0	0.0	0.1	0.1	0.0	0.0	0.0	0.0	0.0	0.0	0.0	0.0	0.0	0.0	0.0	0.0	0.0	0.0	0.0	0.0
+G	-	-	-	-	-	0.6	0.8	0.3	0.8	2.5	2.3	0.0	0.2	0.1	0.5	1.3	0.1	0.3	0.9	0.2	0.0	0.2	0.0	0.2	0.5	0.0	0.1
+G+S	-	-	-	-	-	0.1	0.1	0.1	0.2	1.5	1.5	0.2	0.7	0.0	0.1	0.3	0.0	0.2	0.7	1.1	0.1	0.2	0.2	1.4	0.0	0.1	0.1
+G+S+Hvs	-	-	-	-	-	0.1	0.0	0.1	0.1	1.7	1.7	0.3	0.7	0.1	0.0	0.0	0.0	0.3	0.9	0.5	0.1	0.2	0.1	1.7	0.1	0.1	0.1
-G+B	-	-	-	-	-	0.1	0.3	1.5	0.0	0.1	0.1	0.1	0.2	0.1	0.0	0.3	0.0	0.3	0.0	0.0	0.0	0.5	0.1	0.3	0.1	0.0	0.2
+B	-	-	-	-	-	0.1	0.2	3.0	0.0	0.1	0.1	0.6	0.0	0.0	0.0	0.7	0.0	0.0	0.1	0.2	0.0	0.2	0.1	0.1	0.0	0.0	0.4
+B+G	-	-	-	-	-	0.2	0.4	9.6	0.5	1.8	2.2	3.3	0.1	0.1	0.2	1.5	0.8	0.3	0.9	0.7	0.1	0.1	0.3	1.0	0.1	0.1	0.1
+B+G+S	-	-	-	-	-	0.1	0.1	1.2	0.1	1.4	1.4	4.0	0.4	0.0	0.1	0.3	0.1	0.2	0.7	0.9	0.2	0.1	0.2	1.3	0.2	0.1	0.1
+B+G+S+Hvs	-	-	-	-	-	0.1	0.1	0.2	0.1	1.4	1.5	5.2	0.4	0.1	0.1	0.0	0.3	0.8	1.1	0.1	0.2	0.1	1.4	0.3	0.1	0.2	0.1
-F-G	-	-	-	-	-	0.3	0.1	0.7	0.1	0.2	0.3	0.0	0.1	0.5	0.1	0.0	0.0	0.1	0.1	0.1	0.1	0.1	0.8	0.3	0.1	2.8	0.5
-F	-	-	-	-	-	0.1	0.0	0.0	0.1	0.1	0.1	0.0	0.1	0.2	0.1	0.0	0.1	0.0	0.0	0.0	0.0	0.4	0.2	0.1	1.4	0.4	0.1
-F+G	-	-	-	-	-	0.2	0.3	0.1	0.2	0.7	0.4	0.0	0.0	0.6	0.1	0.7	0.6	1.6	1.9	0.1	0.1	0.0	0.2	0.9	0.2	0.9	0.5
-F+G+S	-	-	-	-	-	0.1	0.0	0.6	0.1	0.3	0.3	0.2	0.2	0.1	0.1	0.2	0.9	1.2	0.5	0.4	0.1	0.1	0.6	0.3	1.8	0.7	
-F+G+S+Hvs	-	-	-	-	-	0.1	0.1	0.3	0.0	0.3	0.3	0.6	0.2	0.1	0.0	0.1	1.0	1.3	0.3	0.4	0.1	0.1	0.6	0.3	0.1	1.8	
-F+G+B	-	-	-	-	-	0.2	0.0	0.9	0.0	0.0	0.2	0.0	0.3	0.1	0.2	0.4	0.0	0.1	0.0	0.0	0.0	0.2	0.0	0.1	0.5	0.1	
-F+B	-	-	-	-	-	0.1	0.1	0.5	0.0	0.1	0.1	0.1	0.0	0.1	0.1	2.2	0.0	0.1	0.0	0.4	0.0	0.1	0.1	0.2	0.1	0.1	
-F+B+G	-	-	-	-	-	0.1	0.2	2.0	0.2	0.7	0.4	0.6	0.1	0.2	0.6	6.8	0.6	1.2	1.8	1.9	0.1	0.0	0.1	0.5	0.4	0.3	
-F+B+G+S	-	-	-	-	-	0.1	0.1	0.6	0.2	0.4	0.4	1.0	0.3	0.1	0.1	0.9	0.2	0.9	1.3	2.8	0.3	0.0	0.1	0.4	0.5	0.2	
-F+B+G+S+Hvs	-	-	-	-	-	0.1	0.1	0.2	0.1	0.4	0.4	1.3	0.4	0.1	0.0	0.2	0.1	0.9	1.4	3.7	0.3	0.1	0.0	0.4	0.6	0.1	

Supplementary table 2. Acquired and in house production of human FcγRs used in SPR experiments.

Name	CD	Allotype	Source	Tag
FcγRIa	CD64	-	Sino Biological	HIS
FcγRIIa	CD32a	131 His	Sino Biological	Biotin
FcγRIIa	CD32a	131 Arg	Sino Biological	Biotin
FcγRIIb	CD32b	-	Sino Biological	Biotin
FcγRIIIa	CD16a	158 Phe	Sino Biological	Biotin
FcγRIIIa	CD16a	158 Val	Sino Biological	Biotin
FcγRIIIb	CD16b	NA2	Sino Biological	HIS
FcγRIIIb	CD16b	NA1	In-house production	Biotin
FcγRIIIb	CD16b	NA2	In-house production	Biotin